The Mitochondrial Thioredoxin System Contributes to the Metabolic Responses Under Drought Episodes in Arabidopsis

Paula da Fonseca-Pereira, Danilo Daloso, Jorge Gago, Franklin Magnum de Oliveira Silva, Jorge Condori-Apfata, Igor Florez-Sarasa, Takayuki Tohge, Jean-Philippe Reichheld, Adriano Nunes-Nesi, Alisdair Fernie, et al.

Article type: Research article

TITLE: The Mitochondrial Thioredoxin System Contributes to the Metabolic Responses Under Drought Episodes in Arabidopsis

Running head: Role of Mitochondrial TRX during drought

***Corresponding author:**

W.L. Araújo

Departamento de Biologia Vegetal,
Universidade Federal de Viçosa,
36570-900 Viçosa, Minas Gerais, Brazil
Email: wlaraujo@ufv.br
Tel: +55 31 3899 2169; Fax: +55 31 3899 2580

Subject areas: (2) environmental and stress responses, and (5) photosynthesis, respiration and bioenergetics.

Number of black and white figures (1), colour figures (7), tables (0)

Number of supplementary Figures (7)

Number of supplementary Tables (3)

Data sets (4)

TITLE: The Mitochondrial Thioredoxin System Contributes to the Metabolic Responses Under Drought Episodes in Arabidopsis

Running head: Role of Mitochondrial TRX during drought

Paula da Fonseca-Pereira[1,2], Danilo M. Daloso[1,§], Jorge Gago[1,3], Franklin Magnum de Oliveira Silva[2], Jorge A. Condori-Apfata[2], Igor Florez-Sarasa[1], Takayuki Tohge[1], Jean-Philippe Reichheld[4], Adriano Nunes-Nesi[2], Alisdair R. Fernie[1], and Wagner L. Araújo[2*]

[1]*Max-Planck-Institut für Molekulare Pflanzenphysiologie, Am Mühlenberg 1, 14476 Potsdam-Golm, Germany*
[2]*Max-Planck Partner Group, Departamento de Biologia Vegetal, Universidade Federal de Viçosa, 36570-900 Viçosa, Minas Gerais, Brazil*
[3]*Research Group on Plant Biology under Mediterranean Conditions, Universitat de les Illes Balears, 07122 Palma de Mallorca, Illes Balears, Spain*
[4]*Laboratoire Génome et Développement des Plantes, Unité Mixte de Recherche 5096, Centre National de la Recherche Scientifique, Université de Perpignan Via Domitia, 66860 Perpignan, France*

***Corresponding author:**

W.L. Araújo
Departamento de Biologia Vegetal,
Universidade Federal de Viçosa,
36570-900 Viçosa, Minas Gerais, Brazil
Email: wlaraujo@ufv.br
Tel: +55 31 3899 2169; Fax: +55 31 3899 2580

Abbreviations: Col-0, Columbia ecotype; DAHP, 3-deoxy-d-*arabino*-heptulosonate 7-phosphate; DRIP2, DREB2A-INTERACTING PROTEIN2; *ETR*, electron transport rate; F_m, maximum chlorophyll fluorescence; F_s, steady-state fluorescence; F_v, variable chlorophyll fluorescence; GC-MS, gas chromatography coupled with mass spectrometry; g_m, mesophyll conductance; LC-MS, liquid chromatography coupled with mass spectrometry; NTR, NADPH-dependent Trx reductase; NTS, NADPH-dependent thioredoxin system; PARi, incident photosynthetically active radiation; PCA, principal component analysis; φPSII, photochemical efficiency of photosystem II; RD 29A, drought responsive A; RD 29B, drought responsive B; RT-PCR, real time PCR; RWC, relative water content; trxo1, thioredoxin o1; TCA, tricarboxylic acid; TW, turgid weight; WT, wild type

Footnotes: [§]Present address: *Departamento de Bioquímica e Biologia Molecular, Universidade Federal do Ceará, Fortaleza, Ceará, Brasil.*

ABSTRACT

Thioredoxins (Trxs) modulate metabolic responses during stress conditions; however the mechanisms governing the responses of plants subjected to multiple drought events and the role of Trxs under these conditions are not well understood. Here we explored the significance of the mitochondrial Trx system in Arabidopsis following exposure to single and repeated drought events. We analyzed the previously characterized NADPH-dependent Trx reductase A and B double mutant (*ntra ntrb*) and two independent mitochondrial thioredoxin o1 (*trxo1*) mutant lines. Following similar reductions in relative water content (~50%) Trx mutants subjected to two drought cycles displayed a significantly higher maximum quantum efficiency (F_v/F_m) and were less sensitive to drought than their wild type counterparts and that all genotypes subjected to a single drought event. Trx mutant plants displayed a faster recovery after two cycles of drought, as observed by the higher accumulation of secondary metabolites and higher stomatal conductance. Our results indicate that plants exposed to multiple drought cycles are able to modulate their subsequent metabolic and physiological response, suggesting the occurrence of an exquisite acclimation in stressed Arabidopsis plants. Moreover, this differential acclimation involves the participation of a set of metabolic changes as well as redox poise alteration following stress recovery.

Keywords: *Arabidopsis thaliana*; metabolic acclimation; mitochondrial Trx system; respiration; tricarboxylic acid cycle; water limitation

Introduction

Limited water availability is the most common environmental stress affecting plant growth and production (Walter et al., 2011). Indeed, it is expected that drought events will become more widespread and severe due to climate changes, affecting plant performance and crop yield (Anjum et al., 2016; Swann et al., 2016; Walter et al., 2011). Hence, a better understanding of how plants respond and acclimate to drought episodes *via* suitable physiological and molecular responses is a fundamental step in the development of stress tolerant crops (Cattivelli et al., 2008; Ding et al., 2013). Therefore, a considerable number of studies have focused on seeking differential responses of plants pre-exposed to dehydration stress treatments in contrast to plants that were not previously stressed (Crisp et al., 2016; Ding et al., 2014, 2013, 2012; Virlouvet et al., 2014; Virlouvet and Fromm, 2015).

It is well established that cell redox homeostasis is disturbed under dehydration stress (Noctor et al., 2014). In addition, one of the important factors determining the effect of water deficit on plant productivity is its impact on mitochondrial respiration (Zivcak et al., 2016). Thus, it is expected that mitochondrial redox proteins can exert a prominent role in drought responses. Accordingly, one of the most important thiol-based enzymes involved in the cellular redox homeostasis management are the thioredoxins (Trxs) (König et al., 2012). Trxs are widely distributed regulatory proteins with two reactive cysteines that confer reductive properties and allow the precise regulation of specific target proteins (Lázaro et al., 2013). In plants, they were early identified as mediators between light-driven electron transport and dark carbohydrate metabolism in chloroplasts (Buchanan, 1980; Mock and Dietz, 2016). In plant mitochondria, and other cellular compartments, a growing

body of information concerning Trx redox regulation has been obtained via the application of proteomics and mass spectrometry-based techniques (Laloi et al., 2001; Balmer et al., 2004; Reichheld et al., 2005; Reichheld et al., 2007; Yoshida et al., 2013; Schmidtmann et al., 2014; Daloso et al., 2015; Møller, 2015). Currently, a functional NADPH-dependent thioredoxin system (NTS) in plants is known to be localized in both cytosol and mitochondria and to be comprised of two highly similar isoforms of NADPH-dependent Trx reductase (NTR), A and B, that are encoded by two distinct genes in Arabidopsis (Laloi et al., 2001; Reichheld et al., 2005). In addition, the extraplastidial NTS is composed of both the subfamily Trx *h* , which is present in the cytosol, nucleus, and mitochondria, and plasma membrane, and the subfamily Trx *o* present in mitochondria and nucleus (Geigenberger et al., 2017). Both subfamilies are, in turn, reduced by NTRA or NTRB.

More than 100 mitochondrial Trx target candidate proteins have been identified by mutant Trx affinity columns in conjunction with proteomics (Balmer et al., 2004; Yoshida et al., 2013). The putative targets are involved in a broad range of mitochondrial processes including photorespiration, ATP synthesis and stress-related reactions. Moreover, tricarboxylic acid (TCA) cycle enzymes and associated pathways were both confirmed as Trx targets *in vitro* and *in vivo* (Daloso et al., 2015; Schmidtmann et al., 2014; Yoshida and Hisabori, 2014). Taken together, these results suggest that mitochondria, similarly to plastids, use TRX and redox status to regulate their main carbon flux pathway (Daloso et al., 2015). In general, TCA cycle enzymes are additionally highly susceptible to oxidative stress (Obata et al., 2011; Winger et al., 2007), which probably involves the participation of the Trx system by mechanisms that are as yet not fully understood. Collectively, this information

suggests an important, albeit somewhat neglected, manner by which mitochondrial metabolism is regulated, in the response to various stresses in plants.

To date, three functional NTRs have been found in Arabidopsis, including the plastidial NTRC, for which a larger number of studies have described its association with plant protection against oxidative stress (Chae et al., 2013; Correa-Aragunde et al., 2015; Lepistö et al., 2013; Moon et al., 2015; Naranjo et al., 2016; Serrato et al., 2004; Spínola et al., 2008). By contrast, the potential significance of NTRA and NTRB under stress conditions remains poorly explored probably due to the functional redundancy between the cytosolic and mitochondrial forms (Geigenberger et al., 2017). This fact apart, it was demonstrated that NTRA- overexpressing plants have a higher stress tolerance against oxidative and drought stresses via the regulation of levels of reactive oxygen species (ROS) (Cha et al. 2014, 2015). In addition, in contrast to *ntra* and *ntrb* single knockout mutants, which show no visible phenotypic modifications under normal conditions, the double *ntra ntrb* mutant exhibited major differences. The *ntra ntrb* plants were characterized as producing wrinkled seeds and exhibiting slow rates of plant growth and accumulating high levels of anthocyanins (Bashandy et al., 2009; Reichheld et al., 2007), which could be expected to increase tolerance to abiotic stresses such as drought (Kovinich et al., 2014; Sperdouli and Moustakas, 2012). Furthermore, a role for Trx *o1* in redox homeostasis during seed germination under salt conditions was recently demonstrated (Ortiz-Espín et al., 2017).

Here we have attempted to characterize the functional role of mitochondrial Trx system following exposure to drought and further investigate whether the re-exposure to a drought event would cause more rapid or stronger metabolic and physiological adjustments. To this end, we evaluated the differential acclimation

mechanisms associated with drought tolerance in mutants of the mitochondrial Trx pathway namely the NADPH-Trx reductase *a* and *b* double mutant (*ntra ntrb*) and the mitochondrially located thioredoxin *o1* (*trxo1*) mutant. Our results demonstrate that the absence of a functional mitochondrial Trx system leads to an enhanced drought tolerance and that following multiple events of drought the Trx system seems to be of key importance.

Results

Mitochondrial Trx mutants under water deficit conditions

To investigate the functional role of the mitochondrial Trx pathway during water shortage, we analyzed the previously characterized *NADP-TRX* reductase *a* and *b* double knockout mutant (*ntra ntrb*) plant that does not express two NTR isoforms localized in cytosol and mitochondria (Reichheld et al., 2007). In addition, we isolated two independent lines that contained T-DNA elements inserted into the thioredoxin o1 (*trxo1*) gene (At2g35010) encoding a mitochondrial Trx from Salk collection (SALK 042792 and SALK 143294) and confirm that transcripts of TRXo1 are absent in these mutant lines (Figure S1).

Following the characterization of the molecular identity of the T-DNA insertional mutants, they were grown alongside wild-type (WT) control plants. There were no visible aberrant phenotypes in the mutants during the vegetative growth under normal watering conditions (Fig. 1A, left panel). In a first experiment, plants cultivated in single pots were exposed to drought stress (Fig. 1). At 10 days after the suspension of irrigation, all the genotypes presented early symptoms of chlorosis and leaf wilting yet WT exhibited more severe dehydration symptoms than the mutants (Fig. 1A, middle panel). To further investigate the development of drought stress symptoms, we next analyzed the relative water content (RWC) and the F_v/F_m (Figs.

1B-C, respectively). During the extended water suspension, all genotypes studied showed similar values of RWC at all the time points evaluated here (Fig. 1B). After 10 days without watering, an important reduction in the RWC was observed for all genotypes, with a water loss of ca. 40% of the initial RWC (Fig. 1B). Moreover, reductions in F_v/F_m values were observed in all genotypes following the cessation of irrigation (Fig. 1C). To assess the capacity of the plants to recover following 10 days of water restriction, irrigation was restored. All genotypes investigated were able to rescue their original RWC (i.e. at day 0, under non-stress condition) after rehydration (Fig. 1B). On the other hand, only the mutant lines *ntra ntrb* and *trxo1-2* showed F_v/F_m values after recovery similar to those observed before the water deficit period (Fig. 1C) indicating that the water availability was enough to fully recover the photosynthetic capacity of these plants. Importantly, WT plants were not able to recover the F_v/F_m values following the restoration of irrigation, suggesting that the Trx mutants were less sensitive to drought stress.

Metabolic changes of Arabidopsis *Trx mutants under water deficit conditions*

In order to obtain a more detailed characterization of the functional significance of the mitochondrial Trx system under water deprivation, we next measured the levels of a broad range of primary (Fig. 2 and Data set I) and secondary (Fig. 3 and Data set II) metabolites in the plants during water deficit treatment. It should be noted that the levels of only relatively few metabolites were significantly different in the mutants in comparison to WT at 0 and 5 days following the onset of drought (Fig. 2 and Data set I). Gas chromatography coupled with mass spectrometry (GC-MS) data revealed that, of the alterations observed under non-stress conditions, all the metabolites that changed significantly in the mutants were lower than the values observed in WT plants, including the decrease in valine in all

mutants and in both serine and lysine in *trxo1-2* mutants. Conversely, as early as 5 days of water deficit, the majority of amino acids increased significantly only in *trxo1-1* plants in relation to WT values. Notably, the majority of the differences in primary metabolites levels was observed at more advanced stress (10 days) and on recovery. Following 10 days without watering, *trxo1-2* mutants showed higher levels of amino acids (alanine, ß-alanine, isoleucine, glutamate, lysine, methionine, ornithine, phenylalanine, serine, threonine, tyrosine, valine and tryptophan), organic acids (ascorbate, fumarate, GABA, glycolate and threonate) and other metabolites such as putrescine and hydroxyproline, when compared to WT plants. In addition, all mutant genotypes showed increased levels of trehalose and raffinose, metabolites that usually accumulate in tolerant plants subjected to desiccation (Arbona et al., 2013; Obata and Fernie, 2012; Valliyodan and Nguyen, 2006). Accordingly, after 10 days of drought, significant changes in a number of secondary metabolites for the mutant lines *trxo1-1* and *trxo1-2* were observed, including decreases in flavonol glycosides (K3G7R and K3R7R), and in the aliphatic glucosinolate 7MTH, in addition to the lower levels of anthocyanin and in the hydroxycinnamates sinapoyl-glucoside (SinG) and di-sinapoyl-glucoside (di-SinG) detected in the three mutants compared to WT plants (Fig. 3 and Data set II). The levels of only one secondary metabolite (7MTH) were significant altered in the *trxo1-1* mutants, while no differences were observed for the other mutants following recovery. On the other hand, a large number of changes in primary metabolites were evident following re-irrigation in the *ntra ntrb* double knockout plants and *trxo1-2* plants, whereas only six metabolites (alanine, arginine, phenylalanine, tyrosine, pyruvate and putrescine) were significantly different in *trxo1-1* plants comparing to WT. Note that there was a general increase in the levels of primary metabolites in all genotypes following both

drought (10 days) and on recovery by comparison to the initial condition (0 day). By contrast to the situation observed following 10 days of drought, there is a clear pattern of down regulation of the majority of the primary metabolites in the mutants following the recovery, compared to WT levels (Fig. 2 and Data set I). For example, the *trxo1-2* and *ntra ntrb* plants displayed lower levels of several amino acids, including aromatic amino acids (phenylalanine, tyrosine and tryptophan) and two branched-chain amino acids (BCAAs), isoleucine and valine, as compared to WT levels. Moreover, the levels of organic acids (GABA, glycerate, pyruvate and threonate), sugars (fructose, mannose, maltose and sorbose), sugar alcohols, such as glycerol and *myo*-inositol were also lower than in WT plants in both *trxo1-2* and *ntra ntrb* mutants on recovery. Double mutant and *trxo1-2* plants were also characterized by lower levels of hydroxyproline and putrescine, while only *ntra ntrb* mutants displayed reductions in spermidine, in comparison to WT on the recovery.

Differential response of Trx mutant plants submitted to single and recurrent drought events

Given the wide range of metabolic changes previously observed in Trx mutant plants exposed to a single drought episode, we next decided to evaluate the responses of plants submitted to a recurrent dehydration stress (Fig. 4). To this end, we performed another experiment with large pots with plants growing side by side and where there was one plant representing each genotype per pot (Fig. 4A). By doing this, we could ensure comparison of the responses in similar soil conditions and to be confident that the water restriction was highly similar across all genotypes.

All genotypes showed similar RWC values under any given condition (Fig. 4B). The RWC was similarly reduced in plants following one (D1) or two (D2) drought events and none of the genotypes was able to fully recover the RWC after re-

irrigation (Fig. 4B). F_v/F_m values (Fig. 4C) were only slightly lower in plants exposed to one (D1) or two (D2) drought events, in comparison to their respective controls (DC). Mutant plants previously exposed to a water suspension event (D2) displayed higher F_v/F_m values than the WT following the same treatment.

Trx-mediated redox regulation seems to be important for stomatal behavior during drought recovery

We further investigated whether gas exchange and chlorophyll *a* fluorescence parameters might be affected in the mutant plants (Table S2 and Figure S3). No differences were observed for any of these parameters in any of the Trx mutants under optimal growth conditions. We next decided to evaluate if the exposure to drought followed by a recovery event could influence these photosynthetic parameters. For this purpose, we analyzed only the photosynthetic responses of re-watered plants (R2) (Table S2), since it was virtually impossible to precisely analyze plants from D1, D2 and R1 due to their very low gas exchange rates ($\Delta CO_2 < 0.5$ in a flow of 100 µmol mol^{-1} air - data not shown). Interestingly, g_s was higher in the mutant lines at R2 compared to their WT counterparts (Table S2 and Figure S3). This indicates that, for the same water losses (Fig. 4B), Trx mutant lines are able to maintain their photosynthetic apparatus close to a normal functionality. In addition, *trxo1-2* plants showed higher chloroplastic CO_2 concentration (C_c). Thus, when taken together, these results indicate a better recovery of g_s in Trx mutant plants following drought conditions.

Differential metabolic responses of Arabidopsis Trx mutants submitted to a repeated drought event compared to not previous stressed plants

We next evaluated the effect of a consecutive stress event in the metabolic response of the plants by measuring the levels of starch, sugars and nitrate at the

middle of the day in illuminated leaves of mutants and WT, as well as a broad range of primary and secondary metabolites. Drought decreased the levels of starch (Figure S4) coupled with increases in the levels of sucrose (Figure S4), glucose (Figure S4) and nitrate in all genotypes analyzed (Figure S5). We also observed a significant decrease in starch (RC) coupled with lower levels of sucrose (R1) and glucose (D2) in the *ntra ntrb* mutant comparing to the WT under the same condition.

By using GC-MS-based metabolite profiling we further observed a remarkable metabolic adjustment in response to the drought treatments (Fig. 5 and Data set III). Overall, the levels of most amino acids and organic acids increased significantly in plants that were subjected to drought stress either once (D1) or twice (D2) and even following re-irrigation (R1 and R2). Compared with WT plants, *ntra ntrb* plants exposed to one single drought event (D1) were characterized by several changes in amino acid levels, including a higher accumulation of asparagine, ornithine and the aromatic amino acids phenylalanine and tryptophan. In addition, we also observed higher levels of tyrosine in all the evaluated mutants and decreases in glutamate in both *ntra ntrb* and *trxo1-1* plants comparing to the WT. Drought induced increases in trehalose (in all mutants), raffinose (*trxo1-1*) and *myo*-inositol (*ntra ntrb*) and reduced the levels of dehydroascorbate (DHA) (*trxo1-2*). Notably, the imposition of a second drought event resulted in alterations in a different set of metabolites. In D2, *ntra ntrb* plants displayed decreases in threonine (also in both *trxo1* lines), citrate, maltose (also in *trxo1-2*) and raffinose compared to the WT. Furthermore, both *trxo-1* lines exhibited increases in DHA levels whereas *trxo1-2* showed increases in tryptophan and galactose levels and *trxo1-1* showed reduction in alanine. Lower levels of putrescine were also found in all mutants at D2.

While a similar number of primary metabolites changed in mutant plants in both drought conditions, D1 and D2, compared to the WT control, a differential response of mutant plants was revealed by liquid chromatography coupled with mass spectrometry (LC-MS) data (Fig. 6 and Data set IV). Thus, only the double *ntra ntrb* mutant exposed to a single drought event (D1) displayed alterations in seven secondary metabolites compared with their respective WT controls. Of these changes, only the hydroxycinnamate SinG1 was reduced, while the other six metabolites (7MSOH, 8MSOO, 4MOI3M, K3GR7R, K3G7R and K3R7R) were increased in *ntra ntrb* plants compared to their respective WT controls. By contrast, a large number of secondary metabolites significantly changed in at least one of Trx mutant plants following two cycles of stress compared to their WT counterparts.

By analyzing primary metabolism following rewatering, it was observed that mutant plants of the R1 condition displayed changes in the levels of more metabolites than R2 plants (Fig. 5 and Data set III). All three Trxs mutants were characterized by lower levels of DHA and higher levels of glycine and hydroxyproline under the R1 condition. Double mutant plants also exhibited decreases in threonate, a known breakdown product of ascorbate (Tsanko S. Gechev et al., 2013) and increases in the shikimate-derivate amino acid tryptophan. Accordingly, ß-alanine and GABA, non-protein amino acids, as well as methionine (also in *trxo1-2*), pyruvate, succinate, serine and spermidine were lower in *ntra ntrb* in comparison to R1 WT plants. In addition, *trxo1-1* plants displayed lower malate and glutamate values, while both *trxo1* mutant lines presented higher alanine levels.

Minor changes were observed in the levels of primary metabolites after a second recovery event (R2). Indeed, only three metabolites were significantly reduced in R2 double *ntra ntrb* mutant plants, namely ß-alanine and maltose, which

were lower in the three mutants, and threonine (which were also lower in *trxo1-1* plants). Moreover, the occurrence of a second drought/recovery cycle induced many changes in the metabolic profile of *trxo1* mutants. The levels of ornithine, erytritol and putrescine were lower in the two *trxo1* mutant lines, whereas we observed higher levels of succinate in *trxo1* lines. Higher levels of galactinol and galactose were also found compared to WT at R2 in *trxo1-1* and *trxo1-2*, respectively.

LC-MS results (Fig. 6 and Data set IV) revealed an accumulation of several secondary metabolites in all mutants following both R1 and R2 conditions in Trx mutants, in comparison with the respective WT control. Interestingly, the levels of 6MTH were higher in all Trx mutants compared to the corresponding WT control in both R1 and R2 conditions, while other secondary metabolites varied in a different way in each situation (R1 or R2). For instance, the levels of the aliphatic GSLs 7MTH and 8MTH were lower in all R1 mutant plants compared to the respective WT, whereas in R2 we observed the opposite (higher levels in the mutants). Lower levels of anthocyanin were observed in *double* and *trxo1-1* mutants in R1 condition and higher levels in *trxo1-2* mutants in R2, compared to their respective WT.

Differential response of pyridine nucleotide content in Arabidopsis *Trx mutants during repeated drought cycles*

We next decided to assay the levels of pyridine nucleotides in the six conditions evaluated here (Figure S6). Interestingly, *ntra ntrb* plants displayed lower levels of NAD^+ and a lower but not significant change in NADH under non stress conditions (DC and RC), compared to the correspondent WT control, which leads to the maintenance of the NADH/NAD^+ ratio in double mutant plants (Figure S6). The levels of NAD^+, $NADP^+$ and NADPH substantially increased in all genotypes following the suspension of watering in both D1 and D2 conditions (Figure S6). Accordingly,

twice drought stressed plants (D2) displayed higher NADH levels than D1 plants. As a result, a clear pattern of reduction in the NADH/NAD^+ ratio (Figure S6) was observed in all D1 plants comparing to both DC and D2 conditions.

Regarding the changes in the NAD(P)H after rehydration, the results showed that plants from neither the R1 nor the R2 condition fully recovered from the previous stress. Thus, the levels of NAD^+, $NADP^+$ and NADPH did not return to the levels displayed by RC plants. In addition, despite the higher NADH levels showed by D2 plants, a great decrease in NADH levels was observed after re-irrigation (R2) in such a way that RC and R2 plants exhibited relatively similar levels of NADH. Moreover, WT plants exposed to a single drought/recovery event (R1) showed greater $NADP^+$ and NAD^+ values than non-stressed WT plants (RC) or even than R2 WT plants. Consequently, all mutant plants displayed lower $NADP^+$ and NAD^+ levels compared with the respective WT (R1), which was significant only for *ntra ntrb* plants. No differences were found for NADPH/$NADP^+$ and NADH/NAD^+ ratios (Figure S6) between the genotypes in any of the evaluated treatments.

Gene expression in TRX mutant plants during repeated drought cycles

We next evaluated the transcriptional responses of select genes through the course of the drought cycle experiment (Fig. 7). Our results demonstrate a significant up-regulation of dehydration-inducible genes, especially the drought-responsive genes, *responsive to desiccation 29A (RD29A)*, *responsive to desiccation 29B (*RD29B) and DREB2A-INTERACTING PROTEIN2 (DRIP2) in drought stressed plants (D1 and D2). Notably, considerably higher transcript levels of RD29A and RD29B were generally found during the second drought cycle (D2) relative to D1 plants. This pattern was also observed following recovery, given the higher

expression of RD29A in R2 plants compared to the R1 plants, which indicates a likely alert state in plants subjected to repeated drought episodes.

Moreover, we followed the expression pattern of the genes encoding for mitochondrial Trx system (TRXo1, NTRA and NTRB). Both TRXo1 and NTRA were higher expressed following two drought cycles in WT plants (D2). Following recovery only NTRA returned to the levels found prior to water stress whereas TRXo1 was even more induced under drought (D2) and recovery (R2) following two drought cycles. By contrast, we did not observe any changes in the expression levels of NTRB following drought or recovery. Although no expression of the related gene was observed for the *trxo1* (both lines *trxo1-1* and *trxo1-2*) and for NTRB in the double knockout, we observed only a strong reduction of NTRA in the double knockout compared with WT levels. Altogether, these results indicate that the genes associated with the mitochondrial Trx system seem to be highly regulated following water stress and that the down-regulation of one most likely culminated with no up-regulation of the others.

Principal Component Analysis reveals specific changes during drought and recovery in Trx Arabidopsis *mutants*

In order to gain a broad overview on the changes that occurred during drought, we subjected the data obtained from plants following cycles of drought to principal component analysis (PCA) and the first and second components was plotted (Fig. 8). Control (DC and RC) and drought (D1 and D2) separated mainly along PC1 (47.0% of data variability), while recovery treatments (R1 and R2) essentially resolved along PC2 (21.4% of data variability). One of the main contributors to the differences observed between control and drought plants were the higher levels of amino acids, which were clearly clustered (Figure S7 and Table S3).

Interestingly, the compatible solutes proline and hydroxyproline were the main determinants of PC1. Both proline and hydroxyproline increased after drought (D1 and D2) and were kept higher following recovery for all the genotypes comparing to control (DC) (Fig. 5 and Data set III). However, proline levels in all mutants do seem to be different from the WT, whereas hydroxyproline was significantly upregulated in all mutants at R1 comparing to their WT counterparts (Fig. 5 and Data set III). The increases in the aromatic amino acids, tyrosine, tryptophan and phenylalanine, as well as in the BCAAs valine and isoleucine were also remarkable within the PC1 where they as well as lysine, serine and alanine provide a massive contribution to sample separation (Figure S7 and Table S3). By contrast, higher levels of GABA and glycine, as well as the strong reductions in glucose, raffinose and galactinol following recovery compared to drought and control plants are seemingly of great importance for the separation observed within PC2.

Discussion

Several suitable physiological, metabolic, and biochemical adjustments are required in order to allow plants to support growth and development under drought. Although the connection between drought and redox metabolism has been demonstrated, our current understanding of the metabolic process associated with mitochondrial redox proteins under stress remains fragmentary. Thus, here we investigated the acclimation responses of mitochondrial TRX mutant plants exposed to drought conditions. By using well-characterized mutants with reduced expression of the mitochondrial Trx system, we observed that these mutants were able to better recover the values of the well-established stress-related F_v/F_m parameter than WT plants after exposure to a single drought event (Fig. 1C). Metabolic changes provide evidence that the absence of a functional mitochondrial Trx system leads to a

complex metabolic reprogramming following dehydration stress (Figs. 2, 3, 5 and 6). Our data also suggest that the mutants most likely displayed a faster recovery due to the operation of other cellular mechanisms in order to compensate the lack of the mitochondrial Trx system and simultaneously maintain cell homeostasis under drought. Our data are thus in good agreement with recent reports which demonstrate that higher activities of antioxidative enzymes are able to counteract TRX*o*1 deficiency in Arabidopsis mutant plants under salinity (Calderón et al., 2018; Ortiz-Espín et al., 2017).

It has been shown that plants are able to fortify their defenses by retaining information from previous stress experiences (Crisp et al., 2016). In good agreement with this, Trx mutants that experienced two cycles of water limitation (D2 plants) responded to water shortage with a significantly higher F_v/F_m (Fig. 4C) and a better visual phenotypic appearance than their counterparts that experienced drought once only (Fig. 4A). Moreover, the levels of sucrose were higher during drought (D1 and D2), but they returned to the levels found prior to water stress following re-irrigation in all genotypes studied here (Figure S4). By contrast, starch levels were virtually depleted after withholding water and were not restored to the values observed at the control condition (Figure S4). Photosynthetic rates (A_N) following re-watering were also not fully recovered at R2 in all genotypes evaluated here despite the similar values of F_v/F_m observed for all genotypes (Table S2). Taken together, these results indicate that stressed plants were not able to fully recover after water limitation.

PCA of the drought cycle experiment revealed that the mutant and WT plants clustered together (Fig. 8), confirming that the metabolic changes triggered by the drought condition followed the same pattern for all genotypes, albeit more pronounced in the mutants (Figs. 5 and 6). The consistent accumulation of aromatic

amino acids in both drought experiments (single and shared pots – Figs. 2 and 5, respectively) likely indicate activation of the phenylpropanoid pathway under water limitation (Dinakar and Bartels, 2013; Tsanko S. Gechev et al., 2013; Jorge et al., 2016). Indeed, larger increases were found in the major classes of secondary metabolites derived from phenylalanine, tyrosine and tryptophan in drought stressed mutant plants than their WT counterparts (Fig. 6 and Data set IV). These results are consistent with the previous demonstration that flavonoid biosynthesis genes and the total flavonoid accumulation are induced in a coordinated manner in the *ntra ntrb* double mutant (Bashandy et al., 2009), and reinforce the idea that secondary metabolism is also subjected to a Trx-mediated redox regulation (Daloso et al., 2015). In fact, it is highly possible that NTRs act on flavonoid biosynthesis through one or several of the cytosolic and/or mitochondrial Trx or Trx-like proteins that are encoded in the Arabidopsis genome (Bashandy et al., 2009). However, despite these evidences, 3-deoxy-d-*arabino*-heptulosonate 7-phosphate (DAHP) synthase, an enzyme of the shikimate pathway, has been the only enzyme of the secondary metabolism demonstrated to be regulated by Trxs (Entus et al., 2002). Future studies are clearly required to identify further Trx-targets from the secondary metabolism and to dissect how and to which extent Trxs coordinate the flux through this pathway.

The results of our secondary metabolism profiles from D1 and D2 plants indicate that a much more extensive number of changes were displayed by Trx mutants subjected to two periods of drought stress (D2) when compared to Trx plants subjected to a single period of drought stress (D1) and to their WT controls (Fig. 6 and Data set IV). This is consistent with the hypothesis that plants are able to incorporate relevant information from previous stress experiences (Hilker et al., 2016; Menezes-Silva et al., 2017; Trewavas, 2003). The results are in good agreement with

the clear higher induction of RD29A and RD29B during the second drought cycle (D2) (Fig. 7), confirming the existence of differential molecular adjustments in D2 plants. It is important to note the alterations in the aromatic sinapoyl-malate (SinM), whose contribution to PC1 was much larger than the average contribution of the other secondary metabolites identified here (Figure S7 and Table S3). SinM is the main sinapate ester in Arabidopsis leaves (König et al., 2014), often described as a classical UV-B screening agent (Dean et al., 2014; Jorge et al., 2016). However, SinM also seems to be associated with drought tolerance in plants (Mattana et al., 2005; Valliyodan and Nguyen, 2006). Not only the increase in amino acid and SinM levels but also other adaptive mechanisms including the accumulation of trehalose (Fig. 2 and Data set I), the polyamines spermidine and putrescine (Figs. 2) and hydroxyproline (Figs. 2 and 5) seem to be of pivotal importance during drought episodes. Accordingly, increases in the levels of all these metabolites have previously been shown to confer drought protection (Cramer et al., 2013, 2007; Do et al., 2013; Jorge et al., 2016; Urano et al., 2009) and as such might be associated with the enhanced performance of Trx mutants following drought. On the other hand, decreases in DHA levels in the Trx mutants in comparison to WT counterparts at R1 (Fig. 5 and Data set III) may suggest alterations in the redox status in these plants, which does not seem to be the case given the absence of differences for $NADPH/NADP^+$ and $NADH/NAD^+$ ratios (Figure S6) between the genotypes in any of the evaluated treatments. Interestingly, tobacco mutant plants overexpressing DHAR (dehydroascorbate reductase) were characterized by lower levels of hydrogen peroxide and DHA in comparison to WT plants, displaying also an increased g_s (Gallie, 2013), which suggest that the lower DHA levels found in Trx mutants (R1) are most likely associated to the better recovery of g_s in the mutants. Furthermore, we

did not observe any evidence of compensation at the expression level of NTR/Trx o1 genes in the mutants investigated here under control conditions (Fig. 7). By contrast, Trx o1 expression was reduced in the *ntra ntrb* double mutant in D2 plants (Fig. 7). Indeed, several other components of the redox metabolism such as glutathione-related enzymes (e.g. glutaredoxins) may be able to compensate the absence of mitochondrial NTR/Trx enzymes. In fact glutathione has been suggested to play a major role in drought stress acclimation (Cheng et al., 2015) and to operates as a backup system for TRX (Reichheld et al 2007; Marty et al 2009; Bashandy et al 2010). Therefore, readjustment of glutathione levels and/or redox state as well as increased activity of glutathione-related enzymes might also be involved in the more complete recovery of *trxo1* and *ntra ntrb* mutants after drought stress, similar to the situation observed in *trxo1* mutants under salt stress (Calderón et al., 2018). However, analysis of this possibility was beyond the scope of the present study and thus remains to be fully investigated.

The higher contribution of the organic acids pyruvate, succinate - metabolites which generally increased in both recovery treatments (R1 and R2) in all genotypes along with the increase in GABA and in the photorespiratory intermediates glycine and glycerate, three metabolites which increased during drought (D1 and D2) and even more following recovery, were associated with the changes observed in our PCA (Fig. 8, Figure S7 and Table S3). The GABA shunt has been associated with energetic stress situations and therefore the changes observed are suggestive that Trx mutants are adjusting their metabolism via changes in the GABA related compounds, in order to support energy production (Fait et al., 2008). This would allow the mutants to better cope with the drought and particularly to recurrent events of water limitation. In turn, the reduction in the abundance of glucose and mannose

together with the accumulation of pyruvate in all genotypes suggest the activation of the glycolytic pathway during recovery (Jorge et al., 2016; Yobi et al., 2013). In addition, the decrease in monosaccharides is linked to the increased production of sucrose (Gechev et al., 2013). However, our data demonstrate a decrease in sucrose following recovery (R1 and R2) compared to the levels observed under drought conditions (D1 and D2) (Figure S5), suggesting the existence of a co-regulation between glycolysis and sucrose metabolism during drought recovery. Similar apparent contrasting metabolite changes have been previously found in response to salt stress and might be attributed to the complex adaptation of soluble osmolytes (Jorge et al., 2016; Obata and Fernie, 2012). The pronounced down-regulation of raffinose and galactinol on recovery indicates that flux was likely redirected to more energetic favorable pathways.

Although our results are not able to fully elucidate the metabolic complexity behind successive drought events it seems that by affecting mitochondrial redox metabolism plants are better able to cope with such situation. We postulate that this is linked with a lower energetic expenditure that would allow a faster recovery in Trx mutants. Collectively, our results are consistent with a complex metabolic reprogramming of the main pathways of primary and secondary metabolism to maintain a fine-tuned and balanced energetic metabolism during drought and recovery. We further demonstrate the existence of a drought memory effect, as observed by the reduced number of changes and a closer metabolic situation in twice-stressed plants (R2) compared to control plants. Perhaps more importantly, we also observed that *trx* mutant plants are less sensitive to such recurrent events and postulate that this is due to a redox-based metabolic reprogramming. It seems likely that a differential and orchestrated response occurred in the mutants, which affected

primary and secondary metabolic pathways and ultimately resulted in alterations in the redox poise following recovery. Thus, increasing our understanding of how Trx interact to allow interorganellar communication will provide us with a more comprehensive picture of redox modulation of both plant growth and metabolism under such conditions. It seems reasonable to assume that the generation of multiple mutants for Trx and glutaredoxin genes localized in different cell compartments will both enhance our knowledge of specificities and redundancies of these different albeit partially complementary redox systems (Geigenberger et al., 2017), allowing us to truly understand the molecular hierarchy under which they operate.

Material and Methods

Growth Conditions and Experimental Design

All *Arabidopsis thaliana* plants were of the Columbia ecotype (Col-0) background. The *ntra ntrb* double-knockout mutant was previously described (Reichheld et al., 2007), whereas the two T-DNA insertion mutants in the trxo1 gene (At2g35010) from the Salk collection *trxo1-1* (SALK_042792) and *trxo1-2* (SALK_143294) were described by Ortiz-Espín et al. 2017. Homozygous lines for each mutant were characterized by genomic PCR (Figure S1). RT-PCR using primer pairs designed to span the T-DNA insertion sites of the two mutant loci was used to investigate transcription of both TRXo1-1 and TRXo1-2 (Figure S1). The Arabidopsis TRXh5 was used as a control to demonstrate the integrity of the RNA preparation. TRXo1-1 and TRXo1-2 mRNAs were detected in the WT (Col-0) using the set of primers 1 (CTCGAGTGATGAAGGGAAATTGGTCG) and 3 (CAACACGTTCTTTACTAGAACGG); however, no amplification products were observed for the transcripts in *trxo1-1* and *trxo1-2* (Figure S1). The seeds of the four genotypes used (Col-0, *ntra ntrb*, *trxo1-1* and *trxo1-2*) were sown on standard greenhouse soil (Stender) in plastic pots with a 0.5-L capacity. The trays containing

the pots were placed under a 12/12-h day/ night cycle (22 /16°C) with 60/75% relative humidity and 150 µmol photons m^{-2} s^{-1} light intensity. Next, 14 days after sowing, plants were transferred to single pots (0.1 L), which were placed in a random arrangement in the tray and then transferred to climate chambers with a 8/16 h day/night cycle (22 /16 °C, 60/75% relative humidity, and 150 µmol photons m^{-2} s^{-1} light intensity). One month after the transference to single pots, plants were subjected to a progressive water deficit by suspension of irrigation and then given recovery irrigation. At days 0, 5 and 10 of drought stress and following 3 days of recovery irrigation, the RWC and the F_v/F_m were determined and whole rosettes were harvested at around 4 h in the light (middle of the photoperiod) for further analysis. Control plants were watered daily and kept under well-watered conditions throughout the whole stress/recovery period.

We additionally grew plants side-by-side in a similar manner in large plastic pots with a 0.5-L capacity to allow comparison of the responses in similar soil conditions and to be confident that the water restriction was identical in all genotypes. To this end, 14 days after sowing, plants were transferred to large pots where there was one plant representing each genotype and kept in climate chambers with similar conditions as described above. One month after the transfer to large pots, plants were divided into three groups. One group was watered daily during the entire experiment including the stress/recovery period (control plants). The second group was subjected to one drought event, followed by a recovery (D1 plants). The third group was submitted to two drought events intercalated with drought recovery periods (D2 plants). The plants subjected to drought events (D1 and D2) and their respective control plants (DC) were all harvested with the same age [with 51 days after sowing (DAS), as indicated by dotted blue lines in the Figure S2]. Similarly, the

plants subjected to the recovery irrigation (R1 and R2) and their respective controls (RC) were all evaluated with the same age (with 54 DAS). Moreover, plants from R2 treatments were subjected to two recurrent episodes of rehydration, each one after 10-day period of drought, while plants from R1 were just once exposed to drought (for 10 days) and recovery (for 3 days). Both experiments were repeated at least twice (and even in different growth facilities) with similar phenotypes observed on each occasion.

Relative water content (RWC)

Leaf RWC was assessed to monitor the status of leaf hydration. One leaf from each replicate was excised and weighed in order to obtain the fresh weight (FW). Afterwards, leaves were hydrated for 2 h in Petri dish containing distilled water, under greenhouse conditions, and weighed in order to obtain the turgid weight (TW). Finally, leaves were oven-dried at 72 °C for 72 h and weighed in order to obtain the dry weight (DW). For the calculation of RWC, the following equation was used: RWC = (FW-DW)/(TW-DW).

Chlorophyll a fluorescence imaging

Fluorescence imaging parameters were determined by using the Imaging-PAM M-Series chlorophyll fluorometer and the software version 2.32 Imaging WIN (both from Heinz Walz GmbH, Effeltrich, Germany). Plants were adapted to darkness for at least 30 min, then the leaves were exposed to a light pulse intensity of 0.5 µmol m^{-2} s^{-1} (1 Hz) to establish the minimum fluorescence image (F_0). Next, a saturating pulse of actinic light (470 nm) of 2400 µmol m^{-2} s^{-1} intensity (10 Hz) was delivered during 0.8 s in order to obtain the maximum fluorescence image (F_m). Thereafter, the calculation of the maximum quantum efficiency of PSII using the formula $F_v/F_m = (F_m - F_0)/F_m$. For semi-quantitative analyses, 15 areas of interest of 1 cm^2 each were

randomly sampled on the image of each leaf. For each parameter, six individual plants were used and the values obtained were averaged.

Gas exchange and chlorophyll a fluorescence measurements

These physiological *in vivo* measurements were performed in the second experiment. One plant of each line and a WT were grown in the same pot (as described previously) taking into account previous considerations to facilitate *in vivo* gas-exchange measurements in the leaves of the growing Arabidopsis rosettes through the 'ice-cream cone-like' soil pot method (Flexas et al., 2007). Leaves (sixth to eighth pair of the rosette) were labeled to perform gas-exchange measurements during the whole experiment. Gas exchange parameters were determined simultaneously with chlorophyll *a* fluorescence measurements using an open-flow infrared gas exchange analyzer system (LI-6400XT; LI-COR) equipped with an integrated fluorescence chamber (LI-6400-40; LI-COR). Instantaneous gas exchange data were obtained after steady-state was reached (40-60 min) under light saturation conditions (1000 µmol photons m^{-2} s^{-1} at the leaf level, while the amount of blue light was set to 10% photosynthetically active photon flux density (PPFD) to optimize stomatal aperture*)*. The reference CO_2 concentration was set at 400 µmol CO_2 mol^{-1} air. All measurements were performed using the 2 cm^2 leaf chamber maintaining block temperature to 25°C, the leaf-to-air vapor pressure deficit was kept at 1.5 to 2.5 kPa ,and flow rates ranging from 100-300 mmol air min^{-1} (depending of gas exchange rates flow was reduced to ensure maximum precision in the equipment following previous recommendations (Gago et al., 2013). Cuvette chamber leakage was corrected as described previously in Flexas et al. 2007. The very low gas-exchange rates under drought conditions did not allow to perform precise measurements with the equipment (Δ CO_2 < 0.5 in a flow of 100 µmol mol^{-1} air). The

same plants used for photosynthesis measurements were darkened for minimum 60 min (at the end of the day) to measure mitochondrial respiration in the dark (R_{dark}); the light non-photorespiratory CO_2 release (R_{light}) was considered as half of R_{dark} (Niinemets et al., 2005). Photorespiration rate (P_r) was calculated following the model based into gas-exchange and chlorophyll fluorescence measurements proposed by Valentini et al. 1995.

In parallel to the gas-exchange measurements, chlorophyll *a* fluorescence recordings were used to calculate the actual photochemical efficiency of photosystem II φPSII = $(F_{m'} - F_s)/F_{m'}$, where F_s is the steady-state fluorescence and $F_{m'}$ is the maximum fluorescence obtained with a saturation pulse of ca. 8000 μmol m^{-2} s^{-1} (Genty et al., 1989). As the ϕPSII represents the number of electrons transferred per photon absorbed in the PSII, the electron transport rate (*ETR*) was calculated as $ETR = \phi PSII * \alpha * ß * PAR_i$, where α is leaf absorbance, ß reflects the partitioning of absorbed quanta between PSII and PSI and PAR_i is the incident photosynthetically active radiation in the leaf surface. The relationship between φPSII and φCO_2 under non-photorespiratory conditions was used to calculate the product α*ß (Valentini et al., 1995). Mesophyll conductance (g_m) was estimated using the method established by Harley et al. 1992. In this method, g_m was estimated using the following equation $g_m = A_N (C_i - (\Gamma^* (J_{flu} + 8(A_N + R_d)))(J_{flu} - 4(A_N + R_d)))$. All parameters, except the CO_2 compensation point (Γ*), were estimated as described above, and Γ* was calculated from *in vitro* determinations of $S_{C/O}$, as $\Gamma^* = 0.5 * O / S_{C/O}$ (Caemmerer, 2000).

Determination of metabolite levels

Whole rosettes were sampled at the indicated time points, immediately frozen in liquid nitrogen, and stored at -80°C until further analysis. Metabolite extraction was performed by rapid grinding in liquid nitrogen and immediate addition of the

appropriate extraction buffer. The levels of starch, sucrose, fructose, and glucose in the leaf tissues were determined exactly as described previously (Fernie et al., 2001). Malate and fumarate were determined exactly as in Nunes-Nesi et al. (2007). Proteins and amino acids were determined as described previously (Cross et al., 2006). Nitrate was determined as detailed in (Sienkiewicz-Porzucek et al., 2010).

Metabolite profiling was determined by GC-MS (primary metabolites) (Lisec et al., 2006) and LC-MS (secondary metabolites) (Tohge and Fernie, 2010). Metabolites were identified by comparison with database entries of authentic standards (Kopka et al., 2005; Schauer et al., 2005). Chromatograms and mass spectra were evaluated by using Chroma TOF 1.0 (Leco, http://www.leco.com/) and TAGFINDER 4.0 software (Luedemann et al., 2008). The relative content of metabolites was calculated by normalization of signal intensity to that of ribitol, which was added as an internal standard and then by dry weight of the material. Secondary metabolite analysis by LC-MS was performed as described (Tohge and Fernie, 2010). All data were processed using Xcalibur 2.1 software (Thermo Fisher Scientific, Waltham, MA, USA). The obtained data matrix of peak area was normalized using the internal standard (isovitexin, CAS: 29702-25-8) and then by dry weight of the material. Metabolite identification and annotation were performed using metabolite databases (Tohge and Fernie, 2009). Identification and annotation of detected peaks followed the recommendations for reporting metabolite data described in Fernie et al. (2011). The full Data set from GC-MS and LC-MS metabolite profiling, including statistical analysis performed as described below, are available as Supporting Information Data sets I-IV.

Determination of pyridine nucleotides

The procedures used to assay pyridine nucleotides were based on the selective hydrolysis of the reduced forms (NADH and NADPH) in acid medium, and of the oxidized forms (NAD^+ and $NADP^+$) in alkaline medium (Hajirezaei et al., 2002). Pyridine nucleotides were assayed using the phenazine methosulfate-catalyzed reduction of dichlorophenolindophenol in the presence of ethanol and alcohol dehydrogenase (for NAD^+ and NADH) or glucose 6-phosphate (G6P) and G6P dehydrogenase (for $NADP^+$ and NADPH) (Queval and Noctor, 2007).

Expression analysis by qRT-PCR

Total RNA was isolated using TRIzol reagent (Ambion, Life Technology) according to the manufacture's recommendations. The total RNA was treated with DNAse I (RQ1 RNase free DNase I, Promega, Madison, WI, USA). The integrity of the RNA was checked on 1% (w/v) agarose gels, and the concentration was measured using a Nanodrop spectrophotometer. Finally, 2 µg of total RNA were reverse transcribed with Superscript II RNase H2 reverse transcriptase (Invitrogen) and oligo (dT) primer according to the manufacture's recommendations. Quantitative real-time PCR were performed in a 96-well plate with an ABI PRISM 7900 HT sequence detection system (Applied Biosystems Appllera, Darmstadt, Germany), using Power SYBR Green PCR Master Mix according to Piques et al., 2009.

The primers used here were designed using the open-source program QuantPrime-qPCR primer designed tool (Arvidsson et al., 2008) The relative transcription abundance was normalized using the constitutively expressed gene FBOX (At5g15710) calculated using the $\Delta\Delta$CT method. The primers used for qRT-PCR were designed using the QuantPrime software (Arvidsson et al., 2008). The primers that were used here are described in the Table S1. Data analyses were

performed as described by Caldana et al., 2007. Four biological replicates were analyzed for each condition.

Statistical analysis

The experiments were conducted in a completely randomized design with 6-8 replicates of each genotype. Data were statistically examined by one-way ANOVA and Tukey's test (P<0.05) using the free software R (2017) with LATTICE library. In order to reduce the dimensionality of the data set and identify the variables that explained a higher proportion of the total variance, a multivariate analysis by Principal Components Analysis (PCA) was used in the Minitab® 17 statistics program (Minitab Inc., Philadelphia). We also used the Thompson tau methods with mean and median to eliminate outliers (Cimbala, 2011), which are data that are statistically inconsistent with the rest of the data.

Funding information

This work was supported by funding from the Max Planck Society, the CNPq (National Council for Scientific and Technological Development, Brazil, Grant 402511/2016-6), and the FAPEMIG (Foundation for Research Assistance of the Minas Gerais State, Brazil, Grant APQ- 01078-15, APQ-01357-14 and RED-00053-16). Scholarship granted by CAPES to PFP, by FAPEMIG to FMOS, by CNPq to JACA, as well as research fellowships granted by CNPq-Brazil to ANN, DMD and WLA are also gratefully acknowledged. JG also acknowledges the financial support from the research program "Juan de la Cierva" post-doc grant from the Spanish Government.

Disclosures

Conflicts of interest: No conflicts of interest declared.

Acknowledgements

The authors acknowledge Ina Krahnert (Max Planck Institute of Molecular Plant Physiology-MPIMP) for helpful technical support.

References

Anjum, N.A., Khan, N.A., Sofo, A., Baier, M., and Kizek, R. (2016) Redox homeostasis managers in plants under environmental stresses. *Frontiers in Environmental Science*. 4: 1–3.

Arbona, V., Manzi, M., de Ollas, C., and Gómez-Cadenas, A. (2013) Metabolomics as a tool to investigate abiotic stress tolerance in plants. *International Journal of Molecular Sciences*. 14: 4885–4911.

Arvidsson, S., Kwasniewski, M., Riaño-Pachón, D.M., and Mueller-Roeber, B. (2008) QuantPrime - a flexible tool for reliable high-throughput primer design for quantitative PCR. *BMC Bioinformatics*. 9: 465.

Balmer, Y., Vensel, W.H., Tanaka, C.K., Hurkman, W.J., Gelhaye, E., Rouhier, N., et al. (2004) Thioredoxin links redox to the regulation of fundamental processes of plant mitochondria. *Proceedings of the National Academy of Sciences*. 101: 2642–2647.

Bashandy, T., Taconnat, L., Renou, J.P., Meyer, Y., and Reichheld, J.P. (2009) Accumulation of flavonoids in an ntra ntrb mutant leads to tolerance to UV-C. *Molecular Plant*. 2: 249–258.

Buchanan, B.B. (1980) Role of light in the regulation of chloroplast enzymes. *Annual Review of Plant Physiology*. 31: 341–374.

Caemmerer, S. Von (2000) Biochemical models of leaf photosynthesis. *Techniques in Plant Sciences*. 53: 1689–1699.

Caldana, C., Scheible, W.-R., Mueller-Roeber, B., and Ruzicic, S. (2007) A quantitative RT-PCR platform for high-throughput expression profiling of 2500 rice transcription factors. *Plant Methods*. 3: 7.

Calderón, A., Sánchez-guerrero, A., Ortiz-Espín, A., Martínez-alcalá, I., Camejo, D., Jiménez, A., et al. (2018) Lack of mitochondrial thioredoxin o1 is compensated by antioxidant components under salinity in Arabidopsis thaliana plants. *Physiologia Plantarum*. doi:10.1111/ppl.12708.

Cattivelli, L., Rizza, F., Badeck, F.W., Mazzucotelli, E., Mastrangelo, A.M., Francia, E., et al. (2008) Drought tolerance improvement in crop plants: an integrated

view from breeding to genomics. *Field Crops Research*. 105: 1–14.

Cha, J.-Y., Barman, D.N., Kim, M.G., and Kim, W.-Y. (2015) Stress defense mechanisms of NADPH-dependent thioredoxin reductases (NTRs) in plants. *Plant Signaling & Behavior*. 10: e1017698. doi: 10.1080/15592324.2015.1017698.

Cha, J.Y., Kim, J.Y., Jung, I.J., Kim, M.R., Melencion, A., Alam, S.S., et al. (2014) NADPH-dependent thioredoxin reductase A (NTRA) confers elevated tolerance to oxidative stress and drought. *Plant Physiology and Biochemistry*. 80: 184–191.

Chae, H.B., Moon, J.C., Shin, M.R., Chi, Y.H., Jung, Y.J., Lee, S.Y., et al. (2013) Thioredoxin reductase type C (NTRC) orchestrates enhanced thermotolerance to arabidopsis by its redox-dependent holdase chaperone function. *Molecular Plant*. 6: 323–336.

Cheng, M.C., Ko, K., Chang, W.L., Kuo, W.C., Chen, G.H., and Lin, T.P. (2015) Increased glutathione contributes to stress tolerance and global translational changes in Arabidopsis. *Plant Journal*. 83: 926–939.

Cimbala, J.M. (2011) Outliers. *Penn State-A Public Reserach University, Department of Mechanical and Nuclear Engineering*. 84.

Correa-Aragunde, N., Cejudo, F.J., and Lamattina, L. (2015) Nitric oxide is required for the auxin-induced activation of NADPH-dependent thioredoxin reductase and protein denitrosylation during root growth responses in arabidopsis. *Annals of Botany*. 116: 695–702.

Cramer, G.R., Ergül, A., Grimplet, J., Tillett, R.L., Tattersall, E.A.R., Bohlman, M.C., et al. (2007) Water and salinity stress in grapevines: Early and late changes in transcript and metabolite profiles. *Functional and Integrative Genomics*. 7: 111–134.

Cramer, G.R., Van Sluyter, S.C., Hopper, D.W., Pascovici, D., Keighley, T., and Haynes, P.A. (2013) Proteomic analysis indicates massive changes in metabolism prior to the inhibition of growth and photosynthesis of grapevine (Vitis viniferaL.) in response to water deficit. *BMC Plant Biology*. 13: 1–22.

Crisp, P.A., Ganguly, D., Eichten, S.R., Borevitz, J.O., and Pogson, B.J. (2016) Reconsidering plant memory: Intersections between stress recovery, RNA turnover, and epigenetics. *Science Advances*. 2: e1501340–e1501340.

Cross, J.M., Korff, M. Von, Altmann, T., Bartzetko, L., Sulpice, R., Gibon, Y., et al.

(2006) Variation of enzyme activities and metabolite levels in 24 Arabidopsis accessions growing in carbon-limited conditions. *Plant Physiology*. 142: 1574–1588.

Daloso, D.M., Müller, K., Obata, T., Florian, A., Tohge, T., Bottcher, A., et al. (2015) Thioredoxin, a master regulator of the tricarboxylic acid cycle in plant mitochondria. *Proceedings of the National Academy of Sciences of the United States of America*. 112: E1392-1400.

Dean, J.C., Kusaka, R., Walsh, P.S., Allais, F., and Zwier, T.S. (2014) Plant sunscreens in the UV-B: ultraviolet spectroscopy of jet-cooled sinapoyl malate, sinapic acid, and sinapate ester derivatives. *Journal of the American Chemical Society*. 136: 14780–14795.

Dinakar, C., and Bartels, D. (2013) Desiccation tolerance in resurrection plants: new insights from transcriptome, proteome and metabolome analysis. *Frontiers in Plant Science*. 4: 482.

Ding, Y., Fromm, M., and Avramova, Z. (2012) Multiple exposures to drought 'train' transcriptional responses in Arabidopsis. *Nature Communications*. 3: 740.

Ding, Y., Liu, N., Virlouvet, L., Riethoven, J.-J., Fromm, M., and Avramova, Z. (2013) Four distinct types of dehydration stress memory genes in Arabidopsis thaliana. *BMC Plant Biology*. 13: 229.

Ding, Y., Virlouvet, L., Liu, N., Riethoven, J.-J., Fromm, M., and Avramova, Z. (2014) Dehydration stress memory genes of Zea mays; comparison with Arabidopsis thaliana. *BMC Plant Biology*. 14: 141.

Do, P.T., Degenkolbe, T., Erban, A., Heyer, A.G., Kopka, J., Köhl, K.I., et al. (2013) Dissecting rice polyamine metabolism under controlled long-term drought stress. *PLoS ONE*. 8: e60325. doi: 10.1371/journal.pone.0060325.

Entus, R., Poling, M., and Herrmann, K. (2002) Redox Regulation of Arabidopsis 3-deoxy- D -arabino- heptulosonate 7-phosphate synthase. *Plant Physiology*. 129: 1866–1871.

Fait, A., Fromm, H., Walter, D., Galili, G., and Fernie, A.R. (2008) Highway or byway: the metabolic role of the GABA shunt in plants. *Trends in Plant Science*. 13: 14–19.

Fernie, A.R., Aharoni, A., Willmitzer, L., Stitt, M., Tohge, T., Kopka, J., et al. (2011) Recommendations for reporting metabolite data. *The Plant Cell*. 23: 2477–2482.

Fernie, A.R., Roscher, A., Ratcliffe, R.G., and Kruger, N.J. (2001) Fructose 2,6-

bisphosphate activates pyrophosphate: Fructose-6-phosphate 1-phosphotransferase and increases triose phosphate to hexose phosphate cycling heterotrophic cells. *Planta*. 212: 250–263.

Flexas, J., Ortuño, M.F., Ribas-Carbo, M., Diaz-Espejo, A., Flórez-Sarasa, I.D., and Medrano, H. (2007) Mesophyll conductance to CO2 in Arabidopsis thaliana. *New Phytologist*. 175: 501–511.

Gago, J., Coopman, R.E., Cabrera, H.M., Hermida, C., Molins, A., Conesa, M.À., et al. (2013) Photosynthesis limitations in three fern species. *Physiologia Plantarum*. 149: 599–611.

Gallie, D.R. (2013) The role of l-ascorbic acid recycling in responding to environmental stress and in promoting plant growth. *Journal of Experimental Botany*. 64: 433–443.

Gechev, T.S., Benina, M., Obata, T., Tohge, T., Sujeeth, N., Minkov, I., et al. (2013) Molecular mechanisms of desiccation tolerance in the resurrection glacial relic Haberlea rhodopensis. *Cellular and Molecular Life Sciences*. 70: 689–709.

Geigenberger, P., Thormählen, I., Daloso, D.M., and Fernie, A.R. (2017) The unprecedented versatility of the plant thioredoxin system. *Trends in Plant Science*. 22: 249–262.

Genty, B., Briantais, J.-M., and Baker, N.R. (1989) The relationship between the quantum yield of photosynthetic electron transport and quenching of chlorophyll fluorescence. *Biochimica et Biophysica Acta (BBA) - General Subjects*. 990: 87–92.

Hajirezaei, M.R., Peisker, M., Tschiersch, H., Palatnik, J.F., Valle, E.M., Carrillo, N., et al. (2002) Small changes in the activity of chloroplastic NADP+-dependent ferredoxin oxidoreductase lead to impaired plant growth and restrict photosynthetic activity of transgenic tobacco plants. *Plant Journal*. 29: 281–293.

Harley, P.C., Loreto, F., Di Marco, G., and Sharkey, T.D. (1992) Theoretical considerations when estimating the mesophyll conductance to CO2 flux by analysis of the response of photosynthesis to CO2. *Plant Physiology*. 98: 1429–1436.

Hilker, M., Schwachtje, J., Baier, M., Balazadeh, S., Isabel, B., Geiselhardt, S., et al. (2016) Priming and memory of stress responses in organisms lacking a nervous system. *Biological Reviews*. 49: 1118–1133.

Jorge, T.F., Rodrigues, J.A., Caldana, C., Schmidt, R., van Dongen, J.T., Thomas-

Oates, J., et al. (2016) Mass spectrometry-based plant metabolomics: metabolite responses to abiotic stress. *Mass Spectrometry Reviews*. 35: 620–649.

König, J., Muthuramalingam, M., and Dietz, K.J. (2012) Mechanisms and dynamics in the thiol/disulfide redox regulatory network: transmitters, sensors and targets. *Current Opinion in Plant Biology*. 15: 261–268.

König, S., Feussner, K., Kaever, A., Landesfeind, M., Thurow, C., Karlovsky, P., et al. (2014) Soluble phenylpropanoids are involved in the defense response of Arabidopsis against *Verticillium longisporum*. *New Phytologist*. 202: 823–837.

Kopka, J., Schauer, N., Krueger, S., Birkemeyer, C., Usadel, B., Bergmüller, E., et al. (2005) GMD@CSB.DB: The Golm metabolome database. *Bioinformatics*. 21: 1635–1638.

Kovinich, N., Kayanja, G., Chanoca, A., Riedl, K., Otegui, M.S., and Grotewold, E. (2014) Not all anthocyanins are born equal: distinct patterns induced by stress in Arabidopsis. *Planta*. 240: 931–940.

Laloi, C., Rayapuram, N., Chartier, Y., Grienenberger, J.M., Bonnard, G., and Meyer, Y. (2001) Identification and characterization of a mitochondrial thioredoxin system in plants. *Proceedings of the National Academy of Sciences of the United States of America*. 98: 14144–14149.

Lázaro, J.J., Jiménez, A., Camejo, D., Iglesias-Baena, I., Martí, M.D.C., Lázaro-Payo, A., et al. (2013) Dissecting the integrative antioxidant and redox systems in plant mitochondria. Effect of stress and S-nitrosylation. *Frontiers in Plant Science*. 4: 1–20.

Lepistö, A., Pakula, E., Toivola, J., Krieger-Liszkay, A., Vignols, F., and Rintamäki, E. (2013) Deletion of chloroplast NADPH-dependent thioredoxin reductase results in inability to regulate starch synthesis and causes stunted growth under short-day photoperiods. *Journal of Experimental Botany*. 64: 3843–3854.

Lisec, J., Schauer, N., Kopka, J., Willmitzer, L., and Fernie, A.R. (2006) Gas chromatography mass spectrometry–based metabolite profiling in plants. *Nature Protocols*. 1: 387–396.

Luedemann, A., Strassburg, K., Erban, A., and Kopka, J. (2008) TagFinder for the quantitative analysis of gas chromatography - Mass spectrometry (GC-MS)-based metabolite profiling experiments. *Bioinformatics*. 24: 732–737.

Mattana, M., Biazzi, E., Consonni, R., Locatelli, F., Vannini, C., Provera, S., et al. (2005) Overexpression of Osmyb4 enhances compatible solute accumulation

and increases stress tolerance of Arabidopsis thaliana. *Physiologia Plantarum*. 125: 212–223.

Menezes-Silva, P.E., Sanglard, L.M.P. V., Ávila, R.T., Morais, L.E., Martins, S.C. V., Nobres, P., et al. (2017) Photosynthetic and metabolic acclimation to repeated drought events play key roles in drought tolerance in coffee. *Journal of Experimental Botany*. 12: 1047–1064.

Mock, H.P., and Dietz, K.J. (2016) Redox proteomics for the assessment of redox-related posttranslational regulation in plants. *Biochimica et Biophysica Acta - Proteins and Proteomics*. 1864: 967–973.

Møller, I.M. (2015) Mitochondrial metabolism is regulated by thioredoxin. *Proceedings of the National Academy of Sciences*. 112: 3180–3181.

Moon, J.C., Lee, S., Shin, S.Y., Chae, H.B., Jung, Y.J., Jung, H.S., et al. (2015) Overexpression of Arabidopsis NADPH-dependent thioredoxin reductase C (AtNTRC) confers freezing and cold shock tolerance to plants. *Biochemical and Biophysical Research Communications*. 463: 1225–1229.

Naranjo, B., Mignée, C., Krieger-Liszkay, A., Hornero-Méndez, D., Gallardo-Guerrero, L., Cejudo, F.J., et al. (2016) The chloroplast NADPH thioredoxin reductase C, NTRC, controls non-photochemical quenching of light energy and photosynthetic electron transport in Arabidopsis. *Plant, Cell & Environment*. 39: 804–822.

Niinemets, Ü., Cescatti, A., Rodeghiero, M., and Tosens, T. (2005) Leaf internal diffusion conductance limits photosynthesis more strongly in older leaves of Mediterranean evergreen broad-leaved species. *Plant, Cell & Environment*. 28: 1552–1566.

Noctor, G., Mhamdi, A., and Foyer, C.H. (2014) The roles of reactive oxygen metabolism in drought: not so cut and dried. *Plant Phisiology*. 164: 1636–1648.

Nunes-Nesi, A., Araújo, W.L., Obata, T., and Fernie, A.R. (2013) Regulation of the mitochondrial tricarboxylic acid cycle. *Current Opinion in Plant Biology*. 16: 335–343.

Nunes-Nesi, A., Carrari, F., Gibon, Y., Sulpice, R., Lytovchenko, A., Fisahn, J., et al. (2007) Deficiency of mitochondrial fumarase activity in tomato plants impairs photosynthesis via an effect on stomatal function. *Plant Journal*. 50: 1093–1106.

Obata, T., and Fernie, A.R. (2012) The use of metabolomics to dissect plant responses to abiotic stresses. *Cellular and Molecular Life Sciences*. 69: 3225–

3243.

Obata, T., Matthes, A., Koszior, S., Lehmann, M., Araújo, W.L., Bock, R., et al. (2011) Alteration of mitochondrial protein complexes in relation to metabolic regulation under short-term oxidative stress in Arabidopsis seedlings. *Phytochemistry*. 72: 1081–1091.

Ortiz-Espín, A., Iglesias-Fernández, R., Calderón, A., Carbonero, P., Sevilla, F., and Jiménez, A. (2017) Mitochondrial AtTrxo1 is transcriptionally regulated by AtbZIP9 and AtAZF2 and affects seed germination under saline conditions. *Journal of Experimental Botany*. 68: 1025–1038.

Piques, M., Schulze, W.X., Höhne, M., Usadel, B., Gibon, Y., Rohwer, J., et al. (2009) Ribosome and transcript copy numbers, polysome occupancy and enzyme dynamics in Arabidopsis. *Molecular Systems Biology*. 5: 314.

Queval, G., and Noctor, G. (2007) A plate reader method for the measurement of NAD, NADP, glutathione, and ascorbate in tissue extracts: application to redox profiling during Arabidopsis rosette development. *Analytical Biochemistry*. 363: 58–69.

Reichheld, J.-P., Khafif, M., Riondet, C., Droux, M., Bonnard, G., and Meyer, Y. (2007) Inactivation of thioredoxin reductases reveals a complex interplay between thioredoxin and glutathione pathways in Arabidopsis development. *The Plant cell*. 19: 1851–1865.

Reichheld, J.P., Meyer, E., Khafif, M., Bonnard, G., and Meyer, Y. (2005) AtNTRB is the major mitochondrial thioredoxin reductase in Arabidopsis thaliana. *FEBS Letters*. 579: 337–342.

Schauer, N., Steinhauser, D., Strelkov, S., Schomburg, D., Allison, G., Moritz, T., et al. (2005) GC-MS libraries for the rapid identification of metabolites in complex biological samples. *FEBS Letters*. 579: 1332–1337.

Schmidtmann, E., König, A.-C., Orwat, A., Leister, D., Hartl, M., and Finkemeier, I. (2014) Redox regulation of Arabidopsis mitochondrial citrate synthase. *Molecular Plant*. 7: 156–169.

Serrato, A.J., Pérez-Ruiz, J.M., Spínola, M.C., and Cejudo, F.J. (2004) A novel NADPH thioredoxin reductase, localised in the chloroplast, which deficiency causes hypersensitivity to abiotic stress in Arabidopsis thaliana. *Journal of Biological Chemistry*. 279: 43821–43827.

Sienkiewicz-Porzucek, A., Sulpice, R., Osorio, S., Krahnert, I., Leisse, A., Urbanczyk-

Wochniak, E., et al. (2010) Mild reductions in mitochondrial NAD-dependent isocitrate dehydrogenase activity result in altered nitrate assimilation and pigmentation but do not impact growth. *Molecular Plant*. 3: 156–173.

Sperdouli, I., and Moustakas, M. (2012) Interaction of proline, sugars, and anthocyanins during photosynthetic acclimation of Arabidopsis thaliana to drought stress. *Journal of Plant Physiology*. 169: 577–585.

Spínola, M.C., Pérez-Ruiz, J.M., Pulido, P., Kirchsteiger, K., Guinea, M., González, M., et al. (2008) NTRC new ways of using NADPH in the chloroplast. *Physiologia Plantarum*. 133: 516–524.

Swann, A.A.L.S., Hoffman, F.M., Koven, C.D., and Randerson, J.T. (2016) Plant responses to increasing CO2 reduce estimates of climate impacts on drought severity. *Proceedings of the National Academy of Sciences*. 113: 10019–10024.

Tohge, T., and Fernie, A.R. (2009) Web-based resources for mass-spectrometry-based metabolomics: A user's guide. *Phytochemistry*. 70: 450–456.

Tohge, T., and Fernie, A.R. (2010) Combining genetic diversity, informatics and metabolomics to facilitate annotation of plant gene function. *Nature Protocols*. 5: 1210–1227.

Trewavas, a (2003) Aspects of plant intelligence. *Annals of Botany*. 92: 1–20.

Urano, K., Maruyama, K., Ogata, Y., Morishita, Y., Takeda, M., Sakurai, N., et al. (2009) Characterization of the ABA-regulated global responses to dehydration in Arabidopsis by metabolomics. *Plant Journal*. 57: 1065–1078.

Valentini, R., Epron, D., Angelis, P.D.E., Matteucci, G., and Dreyer, E. (1995) In situ estimation of net CO2 assimilation, photosynthetic electron flow and photorespiration in Turkey oak (Q. cerris L.) leaves: diurnal cycles under different levels of water supply. *Plant, Cell & Environment*. 18: 631–640.

Valliyodan, B., and Nguyen, H.T. (2006) Understanding regulatory networks and engineering for enhanced drought tolerance in plants. *Current Opinion in Plant Biology*. 9: 189–195.

Virlouvet, L., Ding, Y., Fujii, H., Avramova, Z., and Fromm, M. (2014) ABA signaling is necessary but not sufficient for RD29B transcriptional memory during successive dehydration stresses in Arabidopsis thaliana. *Plant Journal*. 79: 150–161.

Virlouvet, L., and Fromm, M. (2015) Physiological and transcriptional memory in guard cells during repetitive dehydration stress. *New Phytologist*. 205: 596–607.

Walter, J., Nagy, L., Hein, R., Rascher, U., Beierkuhnlein, C., Willner, E., et al. (2011) Do plants remember drought? Hints towards a drought-memory in grasses. *Environmental and Experimental Botany*. 71: 34–40.

Winger, A.M., Taylor, N.L., Heazlewood, J.L., Day, D.A., and Millar, A.H. (2007) Identification of intra- and intermolecular disulphide bonding in the plant mitochondrial proteome by diagonal gel electrophoresis. *Proteomics*. 7: 4158–4170.

Yobi, A., Wone, B.W.M., Xu, W., Alexander, D.C., Guo, L., Ryals, J.A., et al. (2013) Metabolomic profiling in selaginella lepidophylla at various hydration states provides new insights into the mechanistic basis of desiccation tolerance. *Molecular Plant*. 6: 369–385.

Yoshida, K., and Hisabori, T. (2014) Mitochondrial isocitrate dehydrogenase is inactivated upon oxidation and reactivated by thioredoxin-dependent reduction in Arabidopsis. *Frontiers in Environmental Science*. 2: 1–7.

Yoshida, K., Noguchi, K., Motohashi, K., and Hisabori, T. (2013) Systematic exploration of thioredoxin target proteins in plant mitochondria. *Plant and Cell Physiology*. 54: 875–892.

Zivcak, M., Brestic, M., and Sytar, O. (2016) Osmotic adjustment and plant adaptation to drought stress. In: Hossain MA (ed) Drought stress tolerance in plants, vol 1. Springer. International Publishing, Switzerland.

Figure legends:

Fig. 1. Phenotype of Trx Arabidopsis mutants and wild type plants (WT) under drought stress treatment. (A) Images of 4-week-old, short-day-grown Arabidopsis plants immediately (0 days) and after further treatment for 10 days without watering and on recovery irrigation for 3 days. (B) Relative water content (RWC) and (C) the maximum quantum yield of PSII electron transport (F_v/F_m) of leaves of 4-week-old, short-day Arabidopsis plants after further treatment for 0, 5, 10 days without watering and on recovery. Values are means ± SE of five independent samplings. Different letters represent values that were judged to be statistically different between treatments by Tukey´s multiples comparison's test (P<0.05).

Fig. 2. Heat map representing the changes in relative abundance of metabolite levels as measured by GC-MS in Arabidopsis knockout mutants *ntra ntrb*, *trxo1-1* and *trxo1-2*, and wild type plants (WT) after further treatment for 0, 5 and 10 days without watering and on recovery irrigation for 3 days. Relative log2-transformed values of signal intensities were normalized with respect to the mean response calculated for the wild type control at day 0. Values are means ± SE of five independent samplings.

Fig. 3. Heat map representing the changes in relative abundance of secondary metabolite levels as measured by LC-MS in Arabidopsis knockout mutants *ntra ntrb*, *trxo1-1* and *trxo1-2*, and wild type plants (WT) after further treatment for 0, 5 and 10 days without watering and on recovery irrigation for 3 days. Relative log2-transformed values of signal intensities were normalized with respect to the mean response calculated for the wild type control at day 0. Values are means ± SE of five independent samplings. Glucosinolates: 3MSOP, 3-methylsulfinylpropyl glucosinolate; 4MSOB, 4-methylsulfinylbutyl glucosinolate; 5MSOP, 5-methylsulfinylpentyl glucosinolate; 6MSOH, 6-methylsulfinylhexyl glucosinolate; 7MSOH, 7-methylsulfinylheptyl glucosinolate; 8MSOO, 8-methylsulfinyloctyl glucosinolate; 4MTB, 4-methylthiobutyl glucosinolate; 5MTP, 5-methylthiopentyl glucosinolate; 7MTH, 7-methylthioheptyl glucosinolate; 8MTO, 8-methylthiooctyl glucosinolate; I3M, indolyl-3-methyl glucosinolate; 4MI3M, 4-Methoxy-indol-3-ylmethyl-glucosinolate; 1MI3M, 1-Methoxy-3-indolylmethyl glucosinolate. Anthocyanin and flavonol glycosides: A11, anthocynin; Q3GR7R, quercetin-3-O-(2"-O-rhamnosyl)glucoside-7-O-rhamnoside; K3GR7R, kaempferol-3-O-(2"-O-rhamnosyl)glucoside-7-O-rhamnoside; Q3G7R, quercetin-3-O-glucoside-7-O-rhamnoside; K3G7R, kaempferol-3-O-glucoside-7-O-rhamnoside; K3R7R, keampferol-3-O-rhamnoside-7-O-rhamnoside. Hydroxycinnamates and aromatic amino acid: SinG, sinapoyl-glucoside; SinMal; sinapoyl-malate; di-SinG, di-sinapoyl-glucoside.

Fig. 4. Phenotype of Trx Arabidopsis knockout mutants and wild type plants (WT) during dehydration and following rehydration. (A) Images of short-day-grown

Arabidopsis plants immediately (DC and RC) and after further treatment for 10 days without watering (D1 and D2) and on recovery irrigation (R1 and R2) for 3 days. (B) relative water content (RWC) and (C) the maximum quantum yield of PSII electron transport (F_v/F_m) of leaves of short-day-grown Arabidopsis plants. The data represents six conditions: unstressed control (DC), plants drought stressed only once (D1) and twice (D2), unstressed recovery control (RC) and rehydration of plants previously one (R1) or twice (R2) drought stressed. Data represent averages of six biological replicates per genotype and condition. Different letters represent values that that were judged to be statistically different between treatments by Tukey´s multiples comparison's test (P<0.05).

Fig. 5. Heat map representing the changes in relative abundance of primary metabolite levels in Trx Arabidopsis knockout mutants. The genotypes used here were: *ntra ntrb*, *trxo1-1* and *trxo1-2*, and wild type plants (WT) during dehydration and following rehydration as measured by GC-MS. The heat map represents six conditions: unstressed drought control (DC), plants drought stressed only once (D1) and twice (D2), unstressed recovery control (RC) and rehydration of plants previously one (R1) or twice (R2) drought stressed. Data represent averages of six biological replicates per genotype and condition with higher relative expression in mutant lines compared to WT in red and lower expression in blue, as indicated by the scale bar. Metabolites were determined as described in "Materials and Methods." Data are normalized with respect to the mean response calculated for the WT plants at DC.

Fig. 6. Heat map representing the changes in relative abundance of secondary metabolite levels in TRX Arabidopsis knockout mutants. The genotypes used here were: *ntra ntrb*, *trxo1-1* and *trxo1-2*, and wild type plants (WT) during dehydration and following rehydration as measured by LC-MS. The heat map represents six conditions: unstressed drought control (DC), plants drought stressed only once (D1) and twice (D2), unstressed recovery control (RC) and rehydration of plants previously one (R1) or twice (R2) drought stressed. Data represent averages of six biological replicates per genotype and condition with higher relative expression in mutant lines compared to WT in red and lower expression in blue, as indicated by the scale bar. Metabolites were determined as described in "Material and Methods". Data are normalized with respect to the mean response calculated for the WT plants at DC. Glucosinolates: 3MSOP, 3-methylsulfinylpropyl glucosinolate; 4MSOB, 4-methylsulfinylbutyl glucosinolate; 6MSOH, 6-methylsulfinylhexyl glucosinolate; 7MSOH, 7-methylsulfinylheptyl glucosinolate; 8MSOO, 8-methylsulfinyloctyl glucosinolate; 4MTB, 4-methylthiobutyl glucosinolate; 6MTH, 6-methylthiohexyl glucosinolate; 7MTH, 7-methylthioheptyl glucosinolate; 8MTO, 8-methylthiooctyl glucosinolate; I3M, indolyl-3-methyl glucosinolate; 4MOI3M, 4-hydroxy-indolyl-3-

methyl glucosinolate; 1MOI3M, 4-methoxy-indolyl-3-methyl glucosinolate . Hydroxycinnamates: SinG1, sianpoyl-O-glucoside; SinM, sinapoyl-malate; SinGG, sianpoyl-O-di-glucoside. Anthocyanin and flavonol glycosides: A11, anthocynin; Q3GR7R, quercetin-3-O-(2"-O-rhamnosyl)glucoside-7-O-rhamnoside; K3GR7R, kaempferol-3-O-(2"-O-rhamnosyl)glucoside-7-O-rhamnoside; Q3G7R, quercetin-3-O-glucoside-7-O-rhamnoside; K3G7R, kaempferol-3-O-glucoside-7-O-rhamnoside; K3R7R, keampferol-3-O-rhamnoside-7-O-rhamnoside.

Fig. 7. Transcript levels of drought responsive genes (*RD29A*, *RD29B* and *DRIP2*) and of genes related to mitochondrial TRX (*TRXo1*, *NTRA* and *NTRB*) in leaves of Trx Arabidopsis knockout mutants. The genotypes used here were: *ntra ntrb*, *trxo1-1, trxo1-2* and wild type plants (WT) during dehydration and following rehydration. The plants were submitted to five conditions: unstressed drought control (DC), plants drought stressed only once (D1) and twice (D2) and rehydration of plants previously one (R1) or twice (R2) drought stressed. F-BOX was used as an internal control. Data represent averages of four biological replicates per genotype and condition. *RD29A, responsive to desiccation 29A; RD29B*, *responsive to desiccation 29B* and *DRIP2* DREB2A-INTERACTING PROTEIN2 (DRIP2). Different letters represent values that that were judged to be statistically different between treatments by Tukey´s multiples comparison's test (P<0.05).

Fig. 8. Principal component analysis (PCA) of metabolic and growth parameters data. PCA was performed on the correlation matrix of least square means. Numbers in parentheses give the percent variation explained by the first and the second components, which together comprise 68.4% of the total variance. The six treatments are indicated by different colors: unstressed drought control (DC) in black, plants drought stressed only once (D1) in blue and twice (D2) in orange, unstressed recovery control (RC) in pink and rehydration of plants previously one (R1) or twice (R2) drought stressed in green and red, respectively. The colors circles represent the cluster formed by Pearson distance.

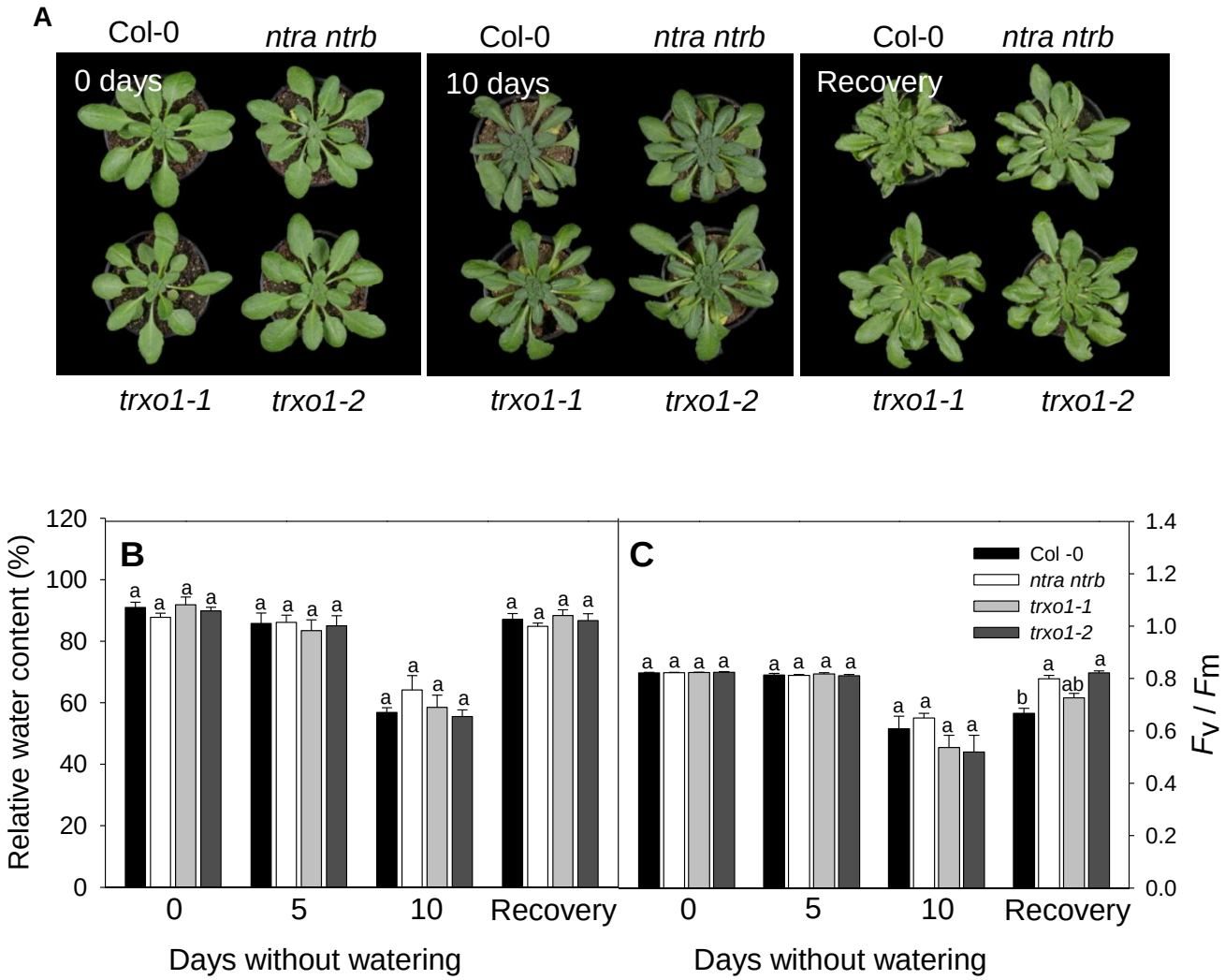

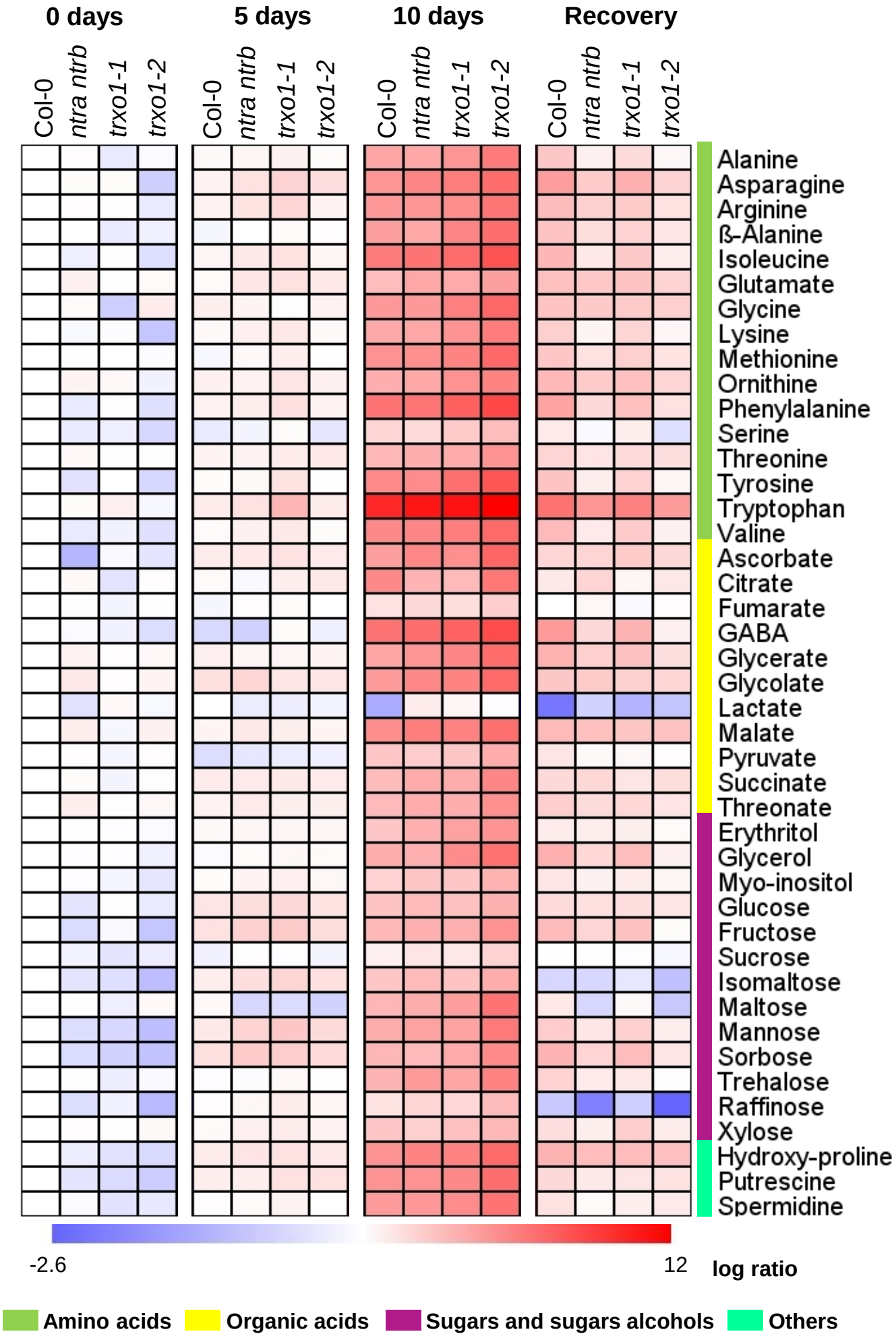

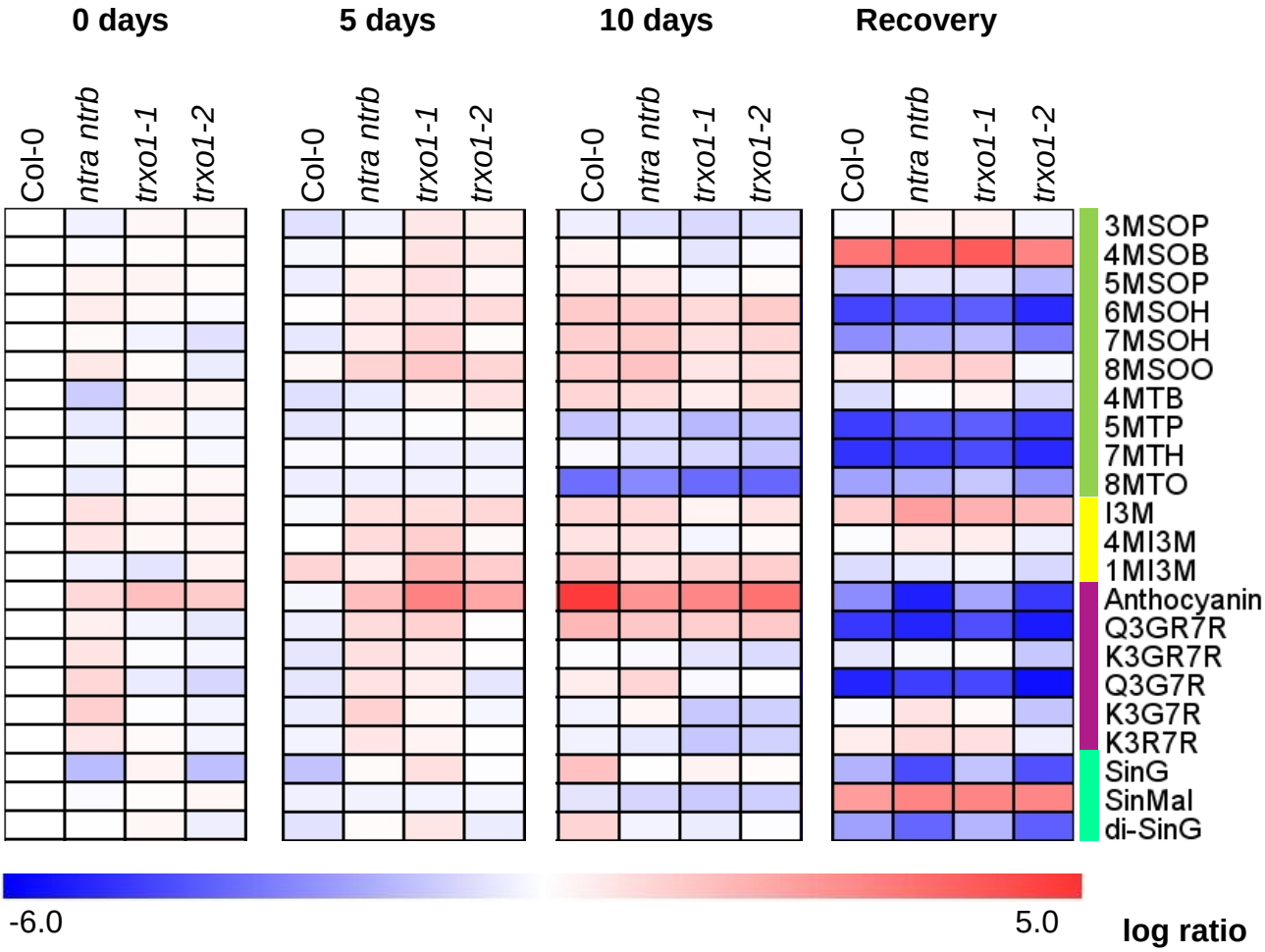

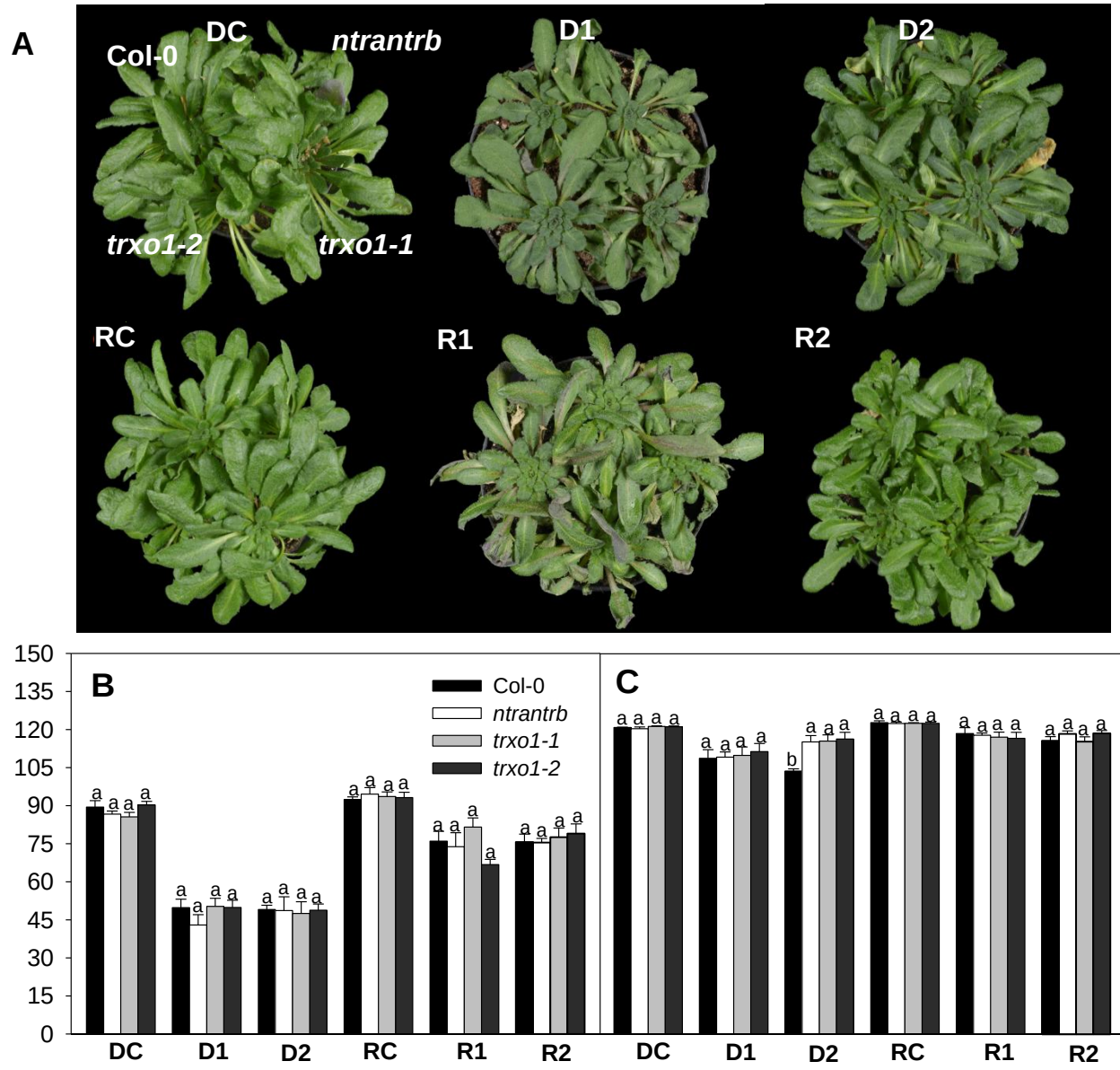

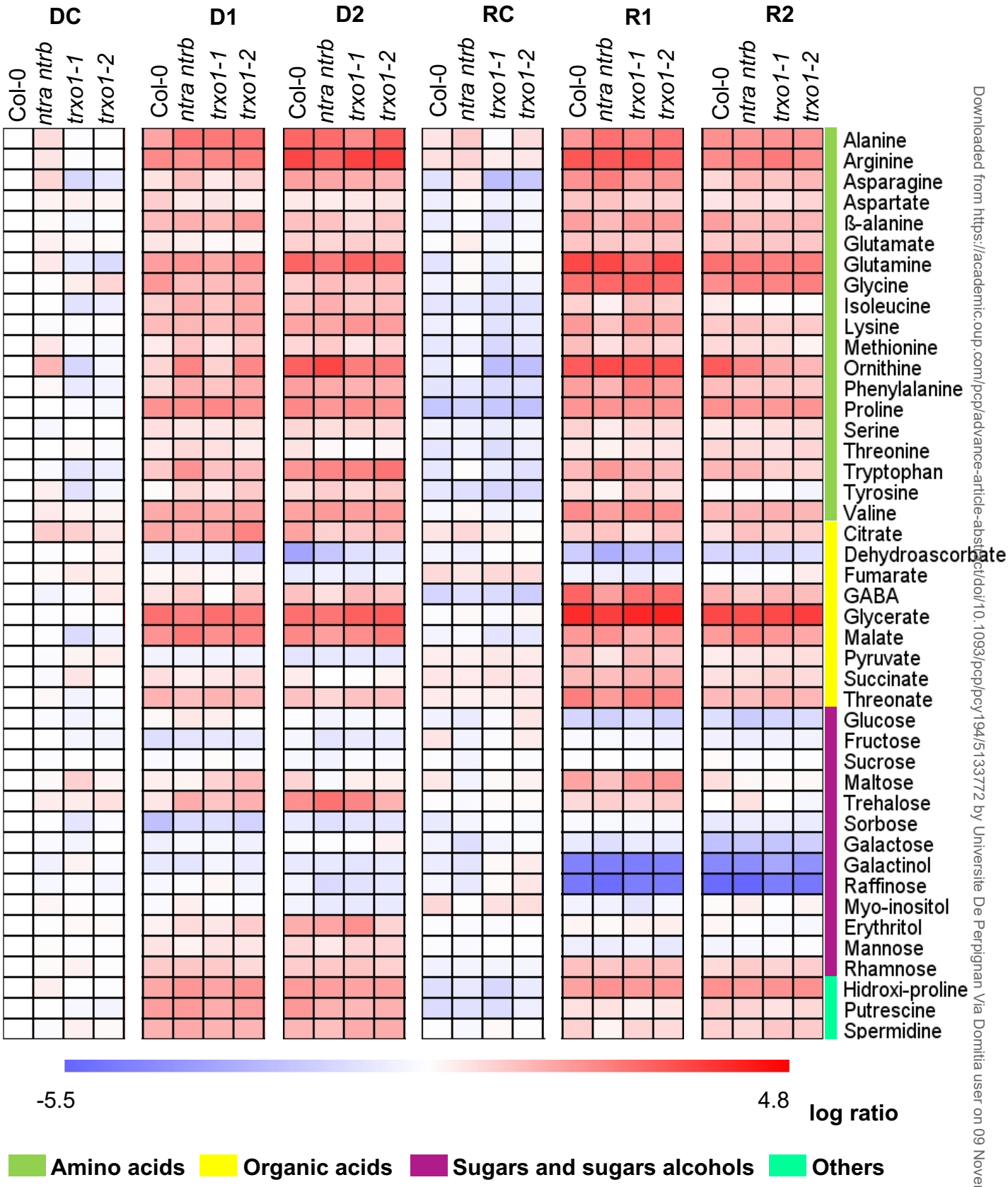

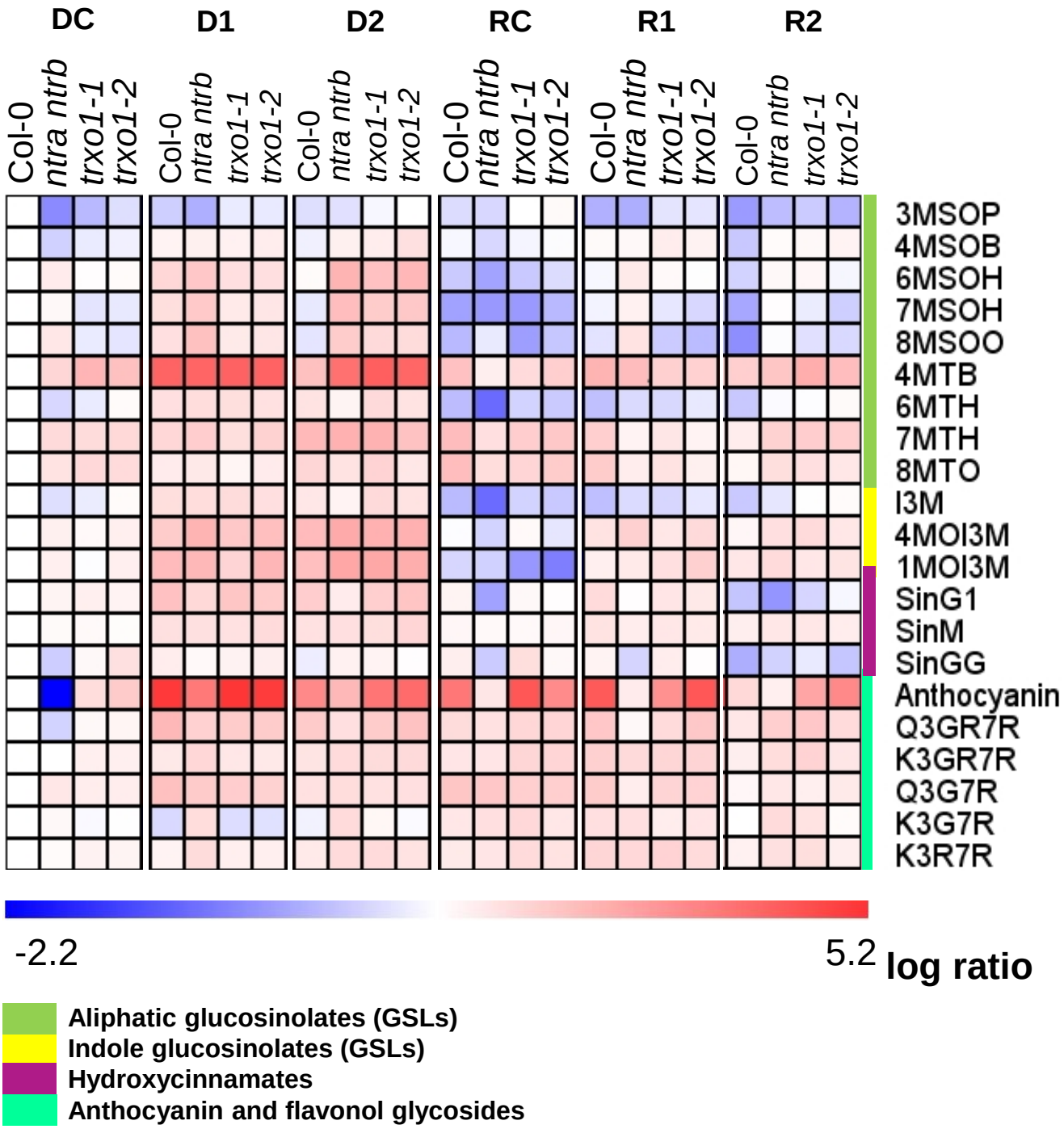

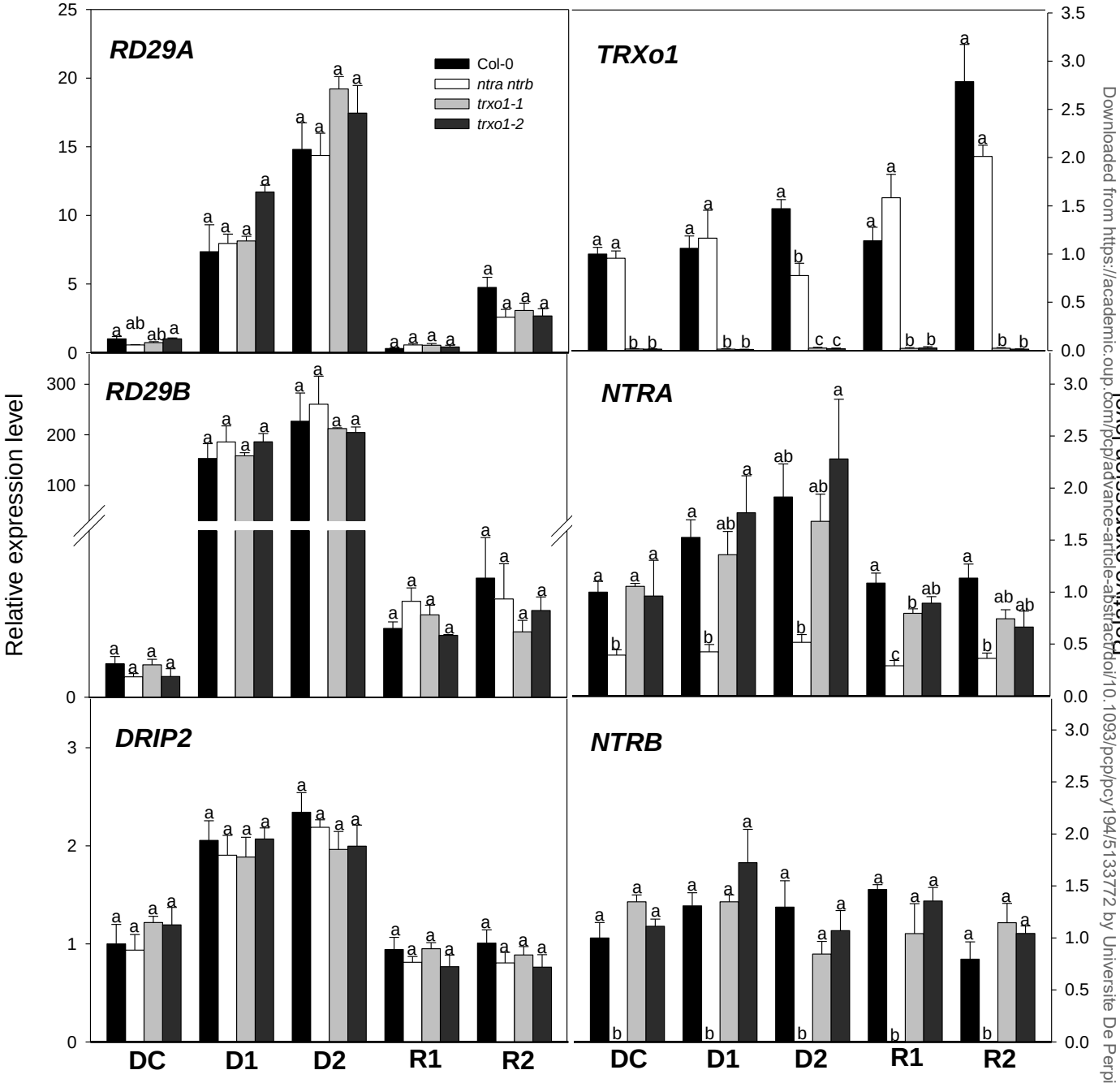

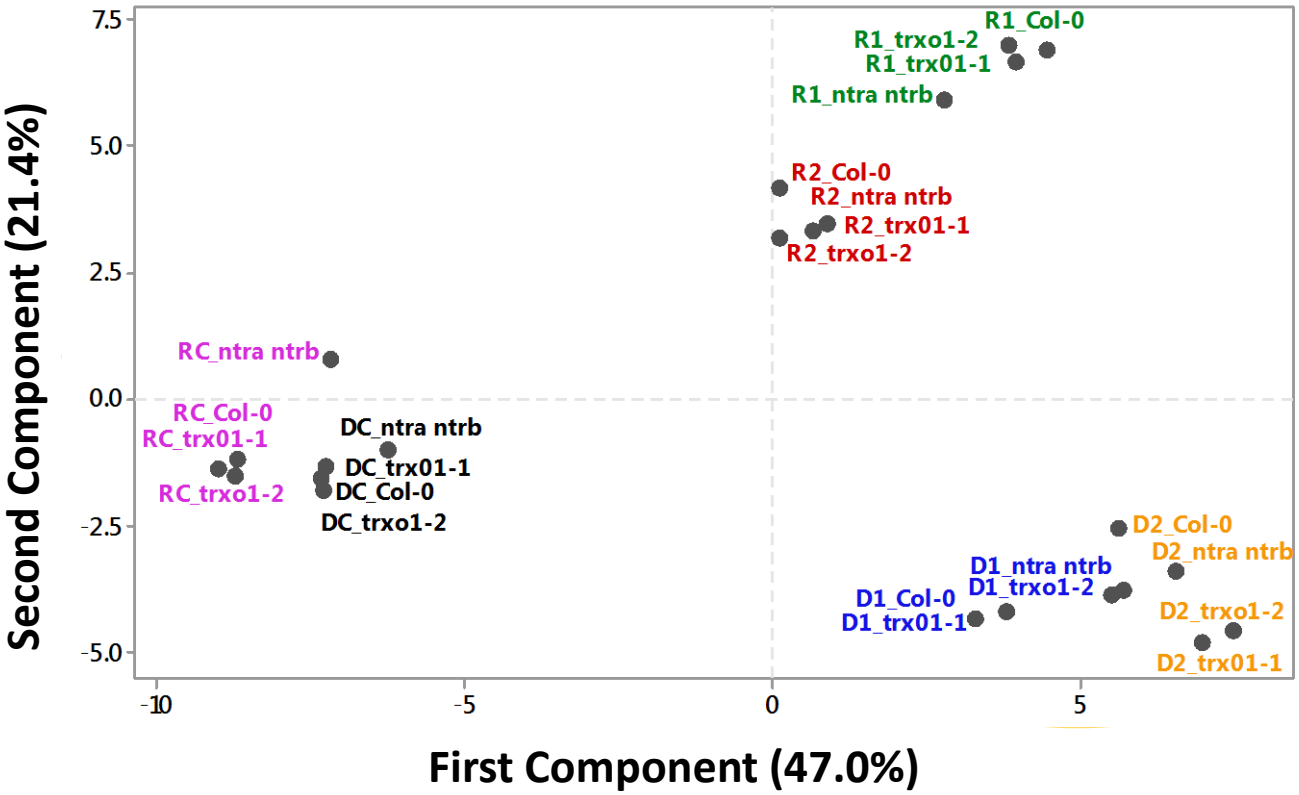

Figure 8. Principal component analysis (PCA) of metabolic and growth parameters data. PCA was performed on the correlation matrix of least square means. Numbers in parentheses give the percent variation explained by the first and the second components, which together comprise 68.4% of the total variance. The six treatments are indicated by different colors: unstressed drought control (DC) in black, plants drought stressed only once (D1) in blue and twice (D2) in orange, unstressed recovery control (RC) in pink and rehydration of plants previously one (R1) or twice (R2) drought stressed in green and red, respectively. The colors circles represent the cluster formed by Pearson distance.